THE JOURNAL OF BIOLOGICAL CHEMISTRY VOL. 281, NO. 44, pp. 33537–33553, November 3, 2006

AKAP79-mediated Targeting of the Cyclic AMP-dependent Protein Kinase to the β_1-Adrenergic Receptor Promotes Recycling and Functional Resensitization of the Receptor*[S]

Received for publication, February 24, 2006, and in revised form, July 18, 2006 Published, JBC Papers in Press, August 28, 2006, DOI 10.1074/jbc.M601809200

Lidia A. Gardner[‡], Steven J. Tavalin[‡], April S. Goehring[§], John D. Scott[§], and Suleiman W. Bahouth[‡1]

From the [‡]Department of Pharmacology, University of Tennessee Health Sciences Center, Memphis, Tennessee 38163 and the [§]Howard Hughes Medical Institute, Vollum Institute, Oregon Health and Science University, Portland, Oregon 97239

Resensitization of G protein-coupled receptors (GPCR) following prolonged agonist exposure is critical for restoring the responsiveness of the receptor to subsequent challenges by agonist. The 3′-5′ cyclic AMP-dependent protein kinase (PKA) and serine 312 in the third intracellular loop of the human β_1-adrenergic receptor (β_1-AR) were both necessary for efficient recycling and resensitization of the agonist-internalized β_1-AR (Gardner, L. A., Delos Santos, N. M., Matta, S. G., Whitt, M. A., and Bahouth, S. W. (2004) *J. Biol. Chem.* 279, 21135–21143). Because PKA is compartmentalized near target substrates by interacting with protein kinase A anchoring proteins (AKAPs), the present study was undertaken to identify the AKAP involved in PKA-mediated phosphorylation of the β_1-AR and in its recycling and resensitization. Here, we report that Ht-31 peptide-mediated disruption of PKA/AKAP interactions prevented the recycling and functional resensitization of heterologously expressed β_1-AR in HEK-293 cells and endogenously expressed β_1-AR in SK-N-MC cells and neonatal rat cortical neurons. Whereas several endogenous AKAPs were identified in HEK-293 cells, small interfering RNA-mediated down-regulation of AKAP79 prevented the recycling of the β_1-AR in this cell line. Co-immunoprecipitations and fluorescence resonance energy transfer (FRET) microscopy experiments in HEK-293 cells revealed that the β_1-AR, AKAP79, and PKA form a ternary complex at the carboxyl terminus of the β_1-AR. This complex was involved in PKA-mediated phosphorylation of the third intracellular loop of the β_1-AR because disruption of PKA/AKAP interactions or small interfering RNA-mediated down-regulation of AKAP79 both inhibited this response. Thus, AKAP79 provides PKA to phosphorylate the β_1-AR and thereby dictate the recycling and resensitization itineraries of the β_1-AR.

The β_1-AR[2] is a major receptor for the physiological regulation of cardiac function by the sympathetic nervous system and plays an important role in clinical management of hypertension and heart failure (2). Agonist-mediated activation of the β_1-AR results in the generation of intracellular cyclic AMP and in the activation of PKA, which in turn phosphorylates numerous intracellular targets that mediate the familiar effects of β-agonists (3). As a consequence of their activation, the β_1-AR and other G protein-coupled receptors (GPCR) can undergo desensitization, which is characterized by attenuation of GPCR signaling intensity (4). The biochemical mechanisms of desensitization are numerous, but appear to be initiated by the phosphorylation of the agonist-occupied GPCR by G protein-coupled receptor kinases (GRK), followed by uncoupling of the GPCR from its cognate G protein by β-arrestins, which culminates in the internalization or sequestration of the GPCR away from its signaling platform (5, 6). Internalization of the GPCR appears to produce different outcomes depending on the type of GPCR and cell line under study. For β_1-AR, β_2-AR, and other GPCR, internalization is a prerequisite for resensitization because intracellular trafficking and subsequent recycling of resensitized GPCR promotes their insertion into the cell membrane to maintain agonist responsiveness (1, 7–9). For the δ-opioid, other GPCRs, the internalized receptors do not recycle back, instead they are retained intracellularly and later degraded either by lysosomal or proteasomal pathways (10–12).

Recently, PKA and its putative substrate, serine at position 312 (Ser^{312}) in the third intracellular loop (3^{rd} IC) of the human β_1-AR, were found to be critical determinants of the ability of the β_1-AR to recycle and resensitize (1). Inhibition of PKA or mutagenesis of Ser^{312} to alanine (S312A) prevented the recycling and resensitization of the agonist-internalized β_1-AR (1). PKA-mediated resensitization of the β_1-AR is termed "homologous resensitization" because PKA is activated through the

* This work was supported by a grant-in-aid from the Southeastern affiliate of the American Heart Association and National Institutes of Health Grants HL-71419 (to S. W. B.), NS-46661 (to S. J. T.), and GM-48231 (to J. D. S.). The costs of publication of this article were defrayed in part by the payment of page charges. This article must therefore be hereby marked "*advertisement*" in accordance with 18 U.S.C. Section 1734 solely to indicate this fact.

[S] The on-line version of this article (available at http://www.jbc.org) contains supplemental movie 1.

[1] To whom correspondence should be addressed: 874 Union Ave., Memphis, TN 38163. Tel.: 901-448-1503; Fax: 901-448-7206; E-mail: sbahouth@utmem.edu.

[2] The abbreviations used are: β_1-AR, β_1-adrenergic receptor; GPCR, G protein-coupled receptors; PKA, cyclic AMP-dependent protein kinase; 3^{rd} IC, third intracellular loop; AKAP, A-kinase anchoring proteins; FRET, fluorescence resonance energy transfer; st-Ht31, stearated Ht31 peptide; GRK, G protein-coupled receptor kinase; WT, wild type; mPKI, myristolated protein kinase inhibitory peptide; FRET*N*, normalized FRET; AMPA, α-amino-3-hydroxy-5-methyl-4-isoxazolepropionic acid; HEK, human embryonic kidney; DMEM, Dulbecco's modified Eagle's medium; CFP, cyan fluorescent protein; YFP, yellow fluorescent protein; siRNA, small interfering RNA; PBS, phosphate-buffered saline; GFP, green fluorescent protein; GST, glutathione *S*-transferase; Tricine, *N*-[2-hydroxy-1,1-bis(hydroxymethyl)ethyl]glycine.

β_1-AR signaling pathway. Therefore, desensitization and resensitization of the β_1-AR are orchestrated through interplay between GRK- and PKA-mediated phosphorylation of this receptor. The involvement of kinases such as GRK, PKA, PKC, and phosphatidylintositol 3-kinase in setting of the trafficking itinerary of GPCR and other cell surface proteins is well established (6, 8). For example, PKA-mediated phosphorylation of the cystic fibrosis transmembrane conductance regulator at Ser^{753} is involved in its recycling, which otherwise is impaired in cystic fibrosis (13). Likewise, PKA is involved in vasopressin-mediated translocation of the water-channel forming protein aquaporin-2 from the intracellular compartment into the plasma membrane, as well as in the trafficking of the AMPA receptor and its insertion into neuronal membranes (14, 15).

PKA is assembled as a tetramer composed of two regulatory (R) and two catalytic (C) subunits. Eukaryotic cells express four isoforms (RI α, β, and RII α, β) of the R subunit and three isoforms (α, β, γ) of the C subunit (16). The RIα and RIIα subunits are ubiquitously expressed, whereas the expression of RIβ and RIIβ is more restricted (16). PKA is a kinase with broad substrate specificity that is involved in numerous biological events (17). The fidelity of PKA-mediated phosphorylation of target proteins is regulated by spatial mechanisms that target PKA toward its substrate and by temporal mechanisms involving phosphodiesterases that degrade cyclic AMP to limit the duration of the biological effects of PKA (18, 19).

The PKA holoenzyme is targeted near potential substrates principally via RII subunit association with AKAPs (20). Each AKAP contains a PKA binding site and a unique subcellular targeting domain that restricts its location within the cell to either unique cellular compartments or specific substrates (20). Many AKAPs serve as organizing centers for signal transduction either by linking upstream signal generators to downstream targets or by recruiting multiple signaling enzymes within signaling hubs (18, 20). In this study, we examined whether the effects of PKA on recycling of the β_1-AR were dependent on PKA anchoring and identified AKAP79 as the specific AKAP involved in recycling and resensitization of the β_1-AR in HEK-293 cells.

EXPERIMENTAL PROCEDURES

Cell Cultures—Human embryonic kidney 293 (HEK-293) cells and neuroepithelioma SK-N-MC cells were obtained from American Type Culture Collection (Manassas, VA). HEK-293 and SK-N-MC cultures were maintained in DMEM with 10% fetal bovine serum (HyClone, Logan, UT). Cortices from 1-day-old rats were dissociated by papain treatment, triturated through Pasteur pipettes, and suspended in media consisting of minimal essential medium with 10% fetal bovine serum and plated at a density of 10^6 cells/ml (21). After 6 h, cells were washed with Neurobasal media with B27 supplement and 0.5 mM L-glutamine.

Construction of FLAG-tagged or Myc-tagged β_1-AR—To allow rapid assessment of cell surface expression of the β_1-AR, the NH_2-terminal initiator methionine was replaced either by the FLAG (DYKDDDDK) or Myc (EQKLISEEDL) sequences, resulting in N-FLAG/Myc-tagged WT β_1-AR. The 8-amino acid FLAG epitope sequence (between parentheses) was inserted at the NH_2 terminus of the β_1-AR by the polymerase chain reaction using a sense primer 5′-AAGCTT(ATGGACTACAAGGACGACGATGACAAG)GGCGCGGGGGGCTCGTCCTGGGCG-3′ and antisense primer 5′-CATGAATTCTACACCTTGGATTCCGAGGCGAAGCCGGG. The Myc tag sequence (between parentheses) was inserted in the NH_2 terminus of the β_1-AR using sense primer 5′-AAGCTTA(ATGGAACAAAAACTCATCTCAGAAGAGGATCTG)GGCGCGGGGGGCTCGTCCTGGGCG-3′ and the antisense primer described earlier. The 1.5-kb β_1-AR cDNA flanked with HindIII (5′) and EcoRI (3′) sites was cloned into the multiple cloning site of mammalian expression vector pcDNA3.1 (Invitrogen). To generate the β_1-AR-(1–424) construct, the full-length β_1-AR cDNA was cut with SmaI and the resulting 1.3-kb cDNA was cloned into pcDNA3.1. Sequences of the epitope-tagged β_1-AR were verified by dideoxy sequencing.

Construction of Fluorescently Tagged β_1-AR, AKAP79, and RIIα Subunit—The coding sequence of the FLAG-tagged WT β_1-AR was amplified by PCR using synthetic oligonucleotides to introduce a 5′ HindIII site, followed by the coding sequence and then by a 3′ BamHI site. The amplification primers for the β_1-AR were: forward primer (5′-AAGCTTATGGACTACAAGGACGACGATGACAAGGGCGCGGGGGTGCTCGTCCTGGGCG) and reverse primer (TGGATCCACCTTGGATTCCGAGGCGAAGCC). The resulting 1.5-kb HindIII-BamHI cDNA was fused in-frame 5′ to the CFP/YFP coding sequence in the pECFP-N1 and pECYFP-N1 vectors (BD Bioscience) to generate NH_2-terminal fusions of the β_1-AR to CFP and YFP. For AKAP79, the coding sequence of human AKAP79 was amplified by PCR using a forward primer (5′-AAGCTTATGGAAACCACAATTTCAGAA) and a reverse primer (3′-TGAATTCTGTAGAAGATTGTTTATTTT) to generate 1.6-kb HindIII-EcoRI cDNA, which was later fused into the pECFP-N1 and pEYFP-N1. Expression of the fusion proteins was confirmed by fluorescence microscopy and Western blot analysis. The cloned sequences were verified by DNA sequencing. Mouse PKA-RIIα in the pECFP and pEYFP vectors (22) was provided by Mark Dell'Acqua (University of Colorado HSC, Denver, CO).

Antibodies, siRNA, Peptides, and Additional Reagents—The antibodies against FLAG (M2) and Myc (9E-10) epitopes were purchased from Sigma and Upstate (Charlottesville, VA), respectively. The monoclonal antibodies to human AKAP79 and to the various subunits of PKA were from BD Bioscience. st-Ht31 and st-Ht31-*pro* peptides were obtained from Promega Corp. The anti-β_1-AR (A-20 and V-19) antibodies were from Santa Cruz Biotechnology (Santa Cruz, CA) and the anti-rat AKAP150 antibody was from Upstate (Charlottesville, VA). AKAP79 siRNA (AAgagaucagcagaagguagu) corresponding to nucleotides 48–66 in human AKAP79 or its scrambled control siRNA (AAggcaacaaaggcuaaguca) and human gravin siRNA (cgaggcggcgccagacaccac) corresponding to nucleotides 161–181 or its scrambled control (ggagcgcggcgaccaacccca) were synthesized by Dharmacon Corp. (Lafayette, CO). siRNAs were transfected at a concentration of 50–100 nM into HEK-293 by the Lipofectamine 2000™ transfection reagent (Invitrogen). After 2 days, cell extracts were probed for AKAP79 or gravin expression by Northern and Western blots. To determine the

effect of the siRNAs on recycling of the WT β_1-AR, cells stably expressing the FLAG-tagged β_1-AR were transiently transfected with 100 nM of each duplex siRNA for 2 days, before conducting the confocal recycling assay described below.

Acid Strip Confocal Recycling Microscopy Protocol—HEK-293 cells stably expressing the FLAG- or Myc-tagged WT β_1-AR were grown on poly-L-lysine-coated glass coverslips and serum-starved at 37 °C for 1 h in DMEM supplemented with 25 mM HEPES, pH 7.4. The receptors were labeled with fluorescein isothiocyanate-conjugated, anti-FLAG M2 IgG (10 μg/ml) for 1 h at 37 °C. Cells were treated with 10 μM isoproterenol for 30 min at 37 °C to promote agonist-mediated receptor internalizaion. Then the cells were chilled in 4 °C Tris-buffered saline to stop endocytosis, and exposed to 0.5 M NaCl, 0.2 M acetic acid (pH 3.5) for 4 min on ice to remove antibody bound to extracellular β_1-AR (1, 15, 23). Cultures were quickly rinsed in warm DMEM supplemented with HEPES, then incubated with 100 μM of the β-antagonist alprenolol at 37 °C for 10, 20, 30, or 45 min to establish the recycle time. After each time period, the coverslips were rinsed and fixed in 4% paraformaldehyde with 4% sucrose in PBS (pH 7.4) for 10 min at room temperature (23).

Analysis of Immunocytochemical Data—Analyses were performed blind to the stimulation history of the culture. Microscope fields had 1–3 cells displaying generally healthy morphology. Six to 10 fields were imaged per culture and $n = 10$ cultures were processed per condition. Confocal fluorescence microscopy was performed using a Zeiss Axiovert LSM 510 (100 × 1.4 DIC oil immersion objective). Fluorescein isothiocyanate was excited with the 488-nm argon laser and imaged through the 520-nm long-pass emission filter. Thresholds were set by visual inspection and kept constant for each condition. Z-stacks of images were exported as TIFF files and individual sections were analyzed with Zeiss LSM 510 and NIH Image 1.6 software as previously described (1).

To determine the distribution of receptors between the membranous and intracellular compartments, a circular boundary was drawn around the inner circumference of all acid/stripped cells to define a 300-nm wide membrane delimited area (24). Fluorescence intensity measurements were calculated in the areas outside and inside the boundary to estimate the membranous *versus* internal pixels. These measurements were repeated in slides with similar threshold settings in which the radii for each boundary did not differ by ±15%. Pixel intensities in the intracellular boundary (internalized β_1-AR) of isoproterenol-treated cells were set arbitrarily as 100% and pixel intensities in the intracellular boundaries of alprenolol-treated cells were calculated as percent of this initial value. In confocal recycling assays, the time constants (τ) for β_1-AR recycling were determined by fitting the percent internal β_1-AR pixel data to a single exponential decay function from $y = y_o + Ae^{-t/\tau}$, where y_o and A are constants. The data are presented as the mean ± S.E.

Dual Confocal Microscopy—HEK-293 cells stably expressing the Myc-tagged β_1-AR were transiently transfected with AKAP79-GFP. The cells were treated with 10 μM isoproterenol for 30 min, acid washed, and then exposed to 100 μM alprenolol for 30 min or 1 h. The coverslips were fixed with 4% paraformaldehyde and stained with Cy3 conjugated to 9E10 anti-Myc tag antibody and visualized by dual confocal microscopy (GFP, $\lambda_{ex} = 488$ nm, $\lambda_{em} = 505–530$ BP; Cy3, $\lambda_{ex} = 543$ nm, $\lambda_{em} = 560$ LP) using LSM-510 multitracking configuration.

FRET Microscopy—These experiments were performed on live or fixed cells using sensitized emission and acceptor photobleaching methods, respectively (25, 26). Double stable cell lines expressing AKAP79-CFP and β_1-AR-YFP, AKAP79-YFP and RII PKA-CFP, and β_1-AR-YFP and RII PKA-CFP were established. In some cases, HEK-293 cells were transfected with the desired plasmids using Lipofectamine for 24–36 h. For live cell microscopy, transiently transfected or double-stable cells were plated onto glass-bottom Petri dishes (Mat-Tek, Ashland, MA) for 24 h and imaged live at room temperature. For fixed cell microscopy, cells were plated on poly-L-lysine-covered coverslips for 24 h. The coverslips were washed with PBS, fixed with 4% paraformaldehyde, pH 7.4, and mounted onto glass slides in Fluoromount G mounting media (Electron Microscopy Sciences, Hatfield, PA). Coverslips were sealed with clear nail polish and imaged within 24 h after fixation.

Sensitized Emission FRET Microscopy—FRET was recorded using the three-channel sensitized emission mode (27, 28). Donor channel (CFP) was acquired using donor excitation (λ = 458 nm) and donor emission (λ = 475–525 nm) with BP filter. Acceptor channel (YFP) was acquired using acceptor excitation (λ = 514 nm) and emission (λ = 530 nm) with LP filter. FRET was acquired using excitation (λ = 458 nm) and emission (λ = 530 nm) with LP filters. Images were taken from donor, acceptor, and FRET samples. Donor and acceptor images were used to evaluate the cross-talk of signals that is caused by image settings and fluorophore properties. The same acquisition parameters were used for donor, acceptor, and FRET samples (28).

FRET Calculations—LSM 510 FRET Macro tool was used to calculate FRET*N* values. FRET*N* is a measure of FRET that is normalized for the concentrations of donor and acceptor fluorophores and therefore represents a fully corrected measure of FRET (27). Quantitative comparisons of different FRET methods has determined that FRET*N* provides the most accurate measure of FRET efficiencies (29). In this method the corrected FRET value for each pixel is calculated and then divided by concentration values for donor and acceptor (27). FRET*N* was calculated on a pixel-by-pixel basis for the entire image and in regions of interest (marked by rectangles) using Equation 1.

$$\mathrm{FRET}N = \frac{\mathrm{FRET1}}{\mathrm{Dfd} \times \mathrm{Afa}} \propto \frac{[\mathrm{bound}]}{[\mathrm{total\ d}] \times [\mathrm{total\ a}]} \qquad \text{(Eq. 1)}$$

The equation indicates the proportional (∝) relationship between FRET*N* and the concentrations of the interacting and noninteracting species. In the equation [*bound*] represents the concentration of interacting pairs of donor labeled species and acceptor labeled species. The values for [*total d*] and [*total a*] represent the total concentrations (interacting and non-interacting) of the donor and acceptor labeled species, respectively. *FRET1* is proportional to the FRET signal from the specimen. *Dfd* is the donor signal that would take place if no FRET occurred and is therefore proportional to the total concentra-

tion of donor. *Afa* is the acceptor signal that would take place if no FRET occurred and is therefore proportional to the total concentration of acceptor.

Donor and acceptor coefficients were determined in the beginning of each experiment and kept the same throughout. Donor, acceptor, and FRET thresholds were set to determine the background value. Threshold values were subtracted from all pixels before FRET calculations. Extreme values were excluded from both, the FRET image as well as data table calculation. FRET*N* images are presented in pseudocolor mode.

Acceptor Photobleaching FRET Microscopy—Changes in the intensity of the donor channel were observed upon complete photobleaching the acceptor (YFP) by a 514-nm argon laser (30). During each photobleaching session, we obtained an image set consisting of time-lapse recordings of donor and acceptor channel intensities. FRET was recorded by examining the quenching of CFP during YFP photobleaching. FRET images were analyzed by the LSM FRET tool version 1.5 (AIM software release 3.2) to calculate the FRET efficiencies using selected area averages for donor CFP before and after bleaching: $FRET_{Efficiency} = (donor\ CFP_{after\ bleaching} - donor\ CFP_{before\ bleaching})/donor\ CFP_{after\ bleaching}$.

Thresholds were set for donor (CFP), acceptor (YFP), and FRET images at the beginning of data collection and the threshold was kept the same for the entire data analysis. FRET efficiencies (%) are presented as mean ± S.E. from 3 to 10 separate acquisition experiments on 5–10 images per experiment.

Effect of Disrupting AKAP-PKA Interactions on the Recycling of the Biotinylated β_1-AR in Neuronal Cells—β_1-AR recycling in human neuroepithelioma SK-N-MC cells and in neonatal rat cortical neurons was measured by the loss of internalized biotinylated β_1-AR. In this assay, the cells were incubated with 50 μM st-Ht31 or st-Ht-31-*pro* for 30 min at 37 °C to inhibit PKA-AKAP interactions. Then cell surface proteins were biotinylated by incubating the cells in ice-cold Hanks' balanced salt solution supplemented with 1.5 mg/ml of sulfo-NHS-SS-biotin (Pierce Biotechnology) for 20 min, followed by quenching of excess biotinylation reagent with glycine. Biotinylated cells were rewarmed to 37 °C in complete culture medium and exposed to isoproterenol for 30 min at 37 °C to induce the internalization of the β_1-AR, followed by chilling of each culture dish on ice to stop membrane trafficking. The remaining surface biotin was quantitatively cleaved with glutathione cleavage buffer (50 mM glutathione in 75 mM NaCl and 10 mM EDTA containing 1% bovine serum albumin and 0.075 N NaOH) twice for 15 min at 4 °C. Cultures were then warmed to 37 °C in complete culture medium containing 10 μM of the β-antagonist alprenolol and 10 μM of each st-Ht31 peptide for 15, 30, and 60 min to allow the internalized β_1-AR to recycle back to the cell surface (1). After each time period, the cells were quickly chilled on ice and incubated for a second time with glutathione cleavage buffer to ensure complete cleavage of any newly appearing (recycled) surface biotin. Then the cells were lysed in radioimmunoprecipitation (RIPA) buffer (150 mM NaCl, 50 mM Tris, pH 8.0, 5 mM EDTA, 1% (v/v) Triton X-100 0.1% SDS, 10 mM NaF, 10 mM Na_2-pyrophosphate, and protease inhibitors). Equal amounts of protein from these cells were mixed with 50 μl of bovine serum albumin-blocked ultralink-neutra avidin beads (Pierce Biotechnology) at 4 °C overnight. The resin was collected by centrifugation, washed several times with lysis buffer, and then extracted with 10 μl/100 μg of input protein of 2× Laemmli sample buffer with 40 mM dithiothreitol at 37 °C for 40 min. The supernatant was subjected to electrophoresis on SDS-containing 4–12% gels, transferred to nitrocellulose, and probed with 1:250 dilution of the anti-β_1-AR antibody and visualized with horseradish peroxidase-conjugated donkey anti-rabbit IgG (GE Healthcare) using the Super Signal detection reagent (Pierce). The density of the M_r 73 kilodaltons β_1-AR from each condition was quantified using a Chemi DOC XRS densitometer (Bio-Rad) equipped with Quantity One software.

Co-immunoprecipitations, Immunoblotting, and Overlay Assays—For co-immunoprecipitations, the cells were washed three times in PBS buffered with 10 mM HEPES, pH 7.5 (H/PBS), then incubated for 30 min at room temperature in cross-linking buffer (H/PBS, 1 mM dithiobis(succinimidyl propionate)) before quenching with H/PBS containing 20 mM glycine. Cells were lysed in RIPA buffer and the insoluble cellular debris was removed by centrifugation at 14,000 × g_{av} for 15 min at 4 °C. After equalizing protein concentrations across all samples, lysates were added to M2 anti-FLAG- or anti-Myc-agarose beads at 4 °C with gentle rotation overnight. Control experiments were performed by incubating lysates with preimmune IgG at the same concentration at 4 °C overnight. Rat brain extracts were prepared by Dounce homogenization in RIPA buffer, followed by clarifying the lysate by centrifugation at 14,000 × g_{av} for 30 min at 4 °C. For each milliliter of lysate, 40 μl of anti-β_1-AR or anti-AKAP79 antibodies were added for ~16 h, then 40 μl of protein G-agarose were added for another 4 h at 4 °C. The immune complexes from all the cells were washed three times in RIPA buffer and eluted from the beads with 2× Laemmli sample buffer containing 100 μM dithiothreitol and 10% 2-mercaptoethanol at 37 °C for 45 min. Resolved proteins and lysate representing between 2 and 5% of input were separated by SDS-PAGE under denaturing conditions and electroblotted to nitrocellulose. Identical gels were run and transferred for separate detection of receptor, AKAP79, or the RII subunits of PKA. AKAP79 and RII subunits were detected with the anti-AKAP79 or anti-RIIα and RIIβ monoclonal antibodies. The β_1-AR in SK-N-MC cells was detected with the A-20 anti-β_1-AR antibody and the β_1-AR in rat brain or neonatal rat cortical neurons was detected with the V-19 anti-β_1-AR antibody. AKAP150 in rat neonatal cortical neurons was detected by the anti-rat AKAP150 antibody from Upstate (Charlottesville, VA).

Far Western and Pulldown Assays—The overlay assay between HEK-293 cell extracts and the ^{32}P-labeled RII α-subunit of PKA were performed as described (31).

The human β_1-AR cDNA was digested with SmaI and XhoI to isolate the 150-bp carboxyl terminus fragment encoding amino acids between 425 and 477. This fragment was cloned in-frame into the glutathione *S*-transferase (GST) pGEX-4T-2 vector (GE Healthcare) and amplified in BL-21 *Escherichia coli* cells. HEK-293 cells that were transfected either with pcDNA 3.1 or Myc-AKAP79 in pcDNA 3.1 were lysed with PBS, 0.2% Triton X-100 supplemented with protease inhibitors. After 16,000 × g_{av} centrifugation of cell lysates, GST or GST-β_1-AR-

(424–477) fusion proteins were added to aliquots of the supernatants. Twenty μl of glutathione-agarose beads (50% slurry in H_2O) were added after mixing for 30 min at 4 °C. The mixture was rotated for another 2 h at 4 °C. After washing three times with the same lysis buffer, the proteins were eluted from beads with sample buffer (containing 2.5% mercaptoethanol). Eluates were separated on a 4–15% gel and analyzed for AKAP79 by immunoblotting.

Adenylyl Cyclase Assays for β-AR Desensitization and Resensitization—HEK-293 cells stably expressing the WT β_1-AR were transiently transfected with 100 nM AKAP79 siRNA or its scrambled control for 2 days. In the experiments using the st-Ht31 peptide, cells expressing the WT β_1-AR were exposed to 50 μM st-Ht31 or st-Ht31-*pro* at 30 min prior to initiating the experiment. For each condition, four identical sets of cells were set up; the first set was used as control for desensitization and the second set for resensitization assays. Cells for desensitization were exposed to 1 mM ascorbic acid (control) or 10 μM isoproterenol for 10 min at 37 °C, and then washed with serum-free DMEM supplemented with 10 mM HEPES and processed for the preparation of membranes as described below. The third set was used as the control for resensitization and the fourth set for resensitization assays. Cells for resensitization were exposed either to 1 mM ascorbic acid (control) or 10 μM isoproterenol for 3 h at 37 °C and then washed with serum-free DMEM supplemented with 10 mM HEPES. The cells were then incubated with 100 μM alprenolol for 1 h at 37 °C, and then washed with serum-free DMEM supplemented with 10 mM HEPES. Membranes were prepared from all cells by hypotonic lysis of the cells with 20 mM HEPES, pH 7.4, 2 mM $MgCl_2$, 1 mM EDTA, and 1 mM 2-mercaptoethanol supplemented with 10 μg/ml leupeptin and 10 μg/ml aprotinin for 10 min on ice. The cells were transferred into a glass-glass homogenizer and lysed by 30 up and down strokes. Cell lysates were centrifuged at 2,500 $\times$ g_{av} for 5 min to pellet the nuclei and the supernatant was centrifuged at 15,000 $\times$ g_{av} for 20 min to pellet the membranes. Then 50 μg of membrane proteins were incubated at 30 °C in a final volume of 0.1 ml containing 50 mM Tris-HCl, pH 7.4, 1 mM $MgCl_2$, 10 mM phosphocreatine, 1 mM cyclic AMP, 2 mM 2-mercaptoethanol, 1 mg/ml bovine serum albumin, 0.4 mM EGTA, 2 mg/ml creatine kinase, 0.2 mM ATP containing 1 μCi of [α-^{32}P]ATP, 1 mM GTP and the various concentrations of isoproterenol. The assay was initiated by the addition of membranes and terminated after 10 min (32). The cyclic AMP that formed was isolated by column chromatography and quantified by liquid scintillation counting. Assays were performed in triplicate and replicated 4 times. The K_{act} ± S.E. for each β_1-AR was calculated using the GraphPad Prism 4 program and statistical comparisons were analyzed using GraphPad Prism 4 and Instat programs.

Phosphorylation and Phosphopeptide Mapping of the β_1-AR—To determine the effect of disrupting AKAP-PKA interactions on isoproterenol-mediated phosphorylation of the β_1-AR, HEK-293 cells expressing the WT β_1-AR were pretreated with 50 μM st-Ht31 or 50 μM st-Ht31-*pro* for 30 min. To determine the effect of down-regulating AKAP79 on isoproterenol-mediated phosphorylation of the β_1-AR, HEK-293 cells expressing the WT β_1-AR were transiently transfected with 100 nM control or AKAP79 siRNA for 2 days. On the day of the experiment, culture plates were switched to phosphate-free DMEM supplemented with 25 mM HEPES, pH 7.4, for 1 h. The medium was supplemented with 200 μCi of $^{32}PO_4$/ml for 1.5 h to label the ATP pools. The cells were stimulated with either 1 mM ascorbic acid or 10 μM isoproterenol in 1 mM ascorbic acid for 10 min at 37 °C. The medium was aspirated and the cells were lysed in RIPA extraction buffer, then centrifuged at 14,000 $\times$ g_{av}. Equivalent amounts of proteins in each supernatant were incubated with M2 anti-FLAG-agarose beads at 4 °C for 5 h. The resins were washed in RIPA buffer, and the proteins were eluted in 2× Laemmli sample buffer supplemented with 40 mM dithiothreitol and resolved by SDS-polyacrylamide gel electrophoresis in 10% gels. The gels were transferred to nitrocellulose in 0.1% sodium vanadate to minimize the dephosphorylation of the receptor during transfer. The amounts of ^{32}P-incorporated into the β_1-AR were determined by densitometric scanning of the blots with Packard Instantimager™. The bands corresponding to phosphorylated β_1-AR protein on the filter were cut out, and submerged in 0.5 ml of 70% (v/v) formic acid containing 100 mg/ml of cyanogen bromide (Science Lab Chemicals, Kingswood, TX) for 1.5 h at room temperature (33). At the end of the digestion, the samples were dried in a SpeedVac concentrator. The dried peptides were dissolved in Tricine sample buffer and subjected to electrophoresis on 16% acrylamide gels in Tricine cathode buffer. The molecular weight of the phosphorylated peptides was determined by electrophoresing alongside the proteolyzed sample a set of pre-stained polypeptides ranging from 26,600 to 1,060 daltons (Sigma, C6210). At the end of the run the gel was electroblotted to nitrocellulose and the filters were counted by the Instantimager, then exposed to an x-ray film overnight (34).

RESULTS

PKA Anchoring Is Essential for Recycling and Resensitization of the Human β_1-AR—To test whether PKA/AKAP interactions are necessary for PKA-mediated recycling of the agonist-internalized β_1-AR, the association between PKA and AKAP was perturbed with the st-Ht31 peptide. st-Ht31 is a cell-permeable peptide that contains the critical RII-binding domain common to all AKAPs and globally disrupts PKA-AKAP interactions, whereas the st-Ht31-*proline* does not disrupt their association and is used as a control (31, 35). Pretreatment of cells expressing the WT β_1-AR with 50 μM st-Ht31 or st-Ht31-*pro* did not interfere with the membranous distribution of the β_1-AR in control cells (Fig. 1*A*, *panels a*, *g*, and *m*). Isoproterenol promoted the internalization of the β_1-AR from clusters of HEK-293 cells and from individual cells pretreated with st-Ht31 (Fig. 1*A*, *panels b*, *h*, and *n*). In the untreated or st-Ht31-*pro*-treated cells, the β_1-AR recycled normally with a $t_{1/2}$ of 18 ± 4 min (Fig. 1, *A*, *panels c–f* and *o–r*, and *B*). Pretreatment with st-Ht31, however, prevented the efficient recycling of the β_1-AR (Fig. 1, *A*, *panels i–l*, and *B*) and the receptors were distributed intracellularly even 4 h after the removal of isoproterenol (data not shown). Therefore, PKA anchoring is required for recycling of the β_1-AR.

To investigate if AKAP-mediated anchoring of PKA exerted an effect on desensitization of the β_1-AR, the effect of st-Ht31

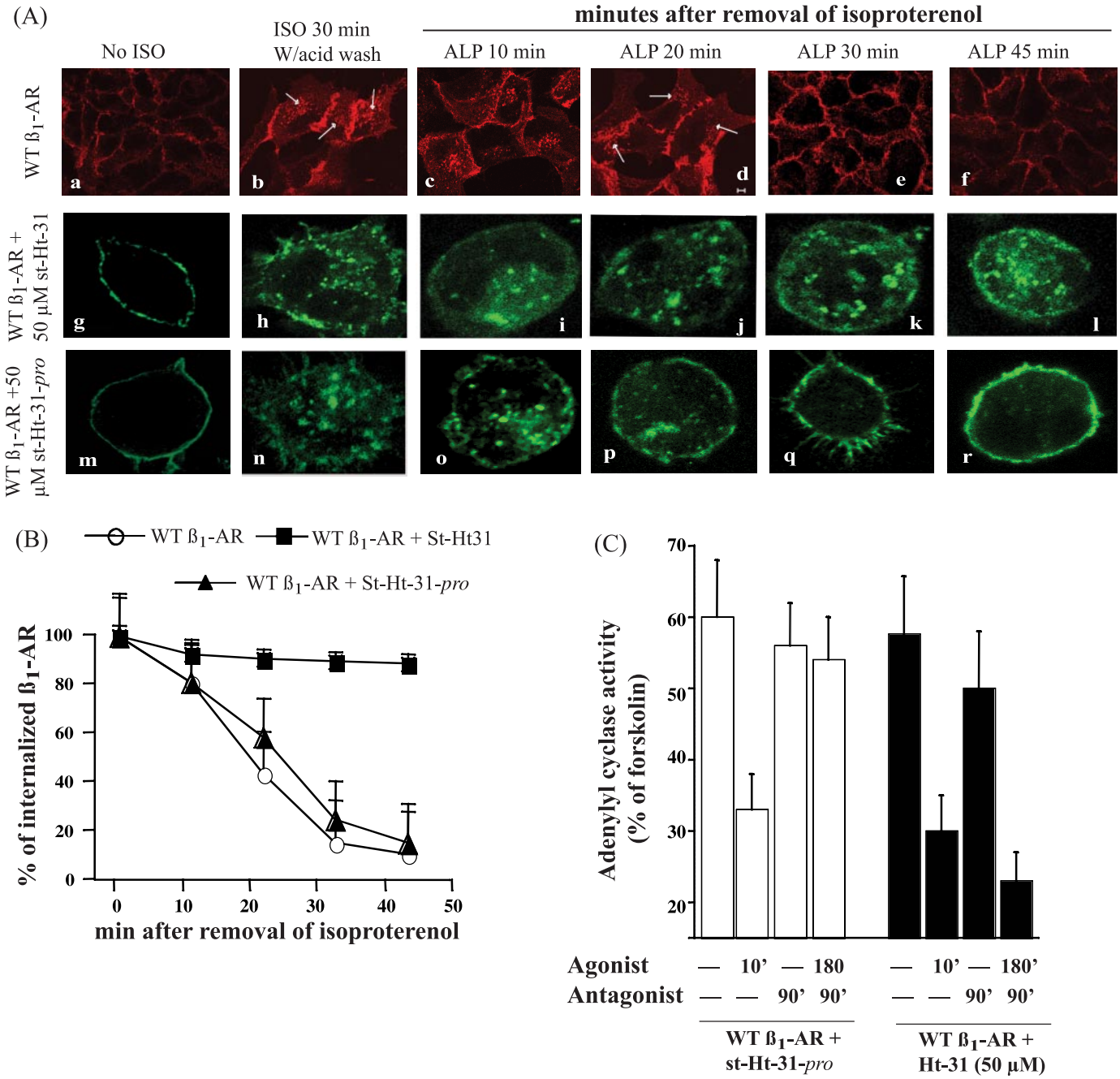

FIGURE 1. **Effect of destabilizing AKAP/PKA interactions on recycling of the agonist-internalized β_1-AR.** *A*, HEK293 cells stably expressing the FLAG-tagged WT β_1-AR were cultured on glass slides and prelabeled for 1 h with fluorescein isothiocyanate anti-FLAG antibody. The cells were incubated with buffer (*panel A*) with 50 μM st-Ht31 (*panel B*) or stHt31-*pro* peptides (*panel C*) for 30 min. These cells were then exposed to 10 μM isoproterenol for 30 min, then acid washed to strip the fluorescent label from non-internalized receptors. After adding alprenolol (100 μM) and 20 μM of each peptide, the slides were fixed at the indicated times and visualized by confocal microscopy ($n = 3$). Each *scale bar* represents 5 μm. *B*, the pixels inside a 300-nm boundary in isoproterenol/acid-washed cells were set arbitrarily to 100% to indicate 100% internalization and the ratios in alprenolol-treated cells were calculated and expressed as % for each time period. The $t_{0.5}$ for recycling was calculated by fitting the relevant data to a single exponential function of time from $y = y_o + A(1 - e^{-t/\tau})$, where y_o and A are constants. *C*, cells expressing WT β_1-AR were pretreated with 50 μM st-Ht31 or st-Ht31-*pro* for 30 min, then exposed to buffer or 10 μM isoproterenol for either 10 min or 3 h at 37 °C. For the 3-h condition, the buffer or isoproterenol were replaced with 100 μM of the β-adrenergic antagonist propranolol for 1.5 h. The ratios for the specific activity of adenylyl cyclase in membranes exposed to isoproterenol to those exposed to forskolin were used to determine the percentile of maximal adenylyl cyclase activity in each type of membrane. These experiments were replicated ($n = 4$) each in triplicate to determine the S.E.

or st-Ht31-*pro* on adenylyl cyclase activity in response to acute isoproterenol treatment was determined. In this assay, rapid desensitization of adenylyl cyclase in membranes prepared from cells pre-exposed to st-Ht31 or st-Ht31-*pro* was observed after 10 min of exposing the cells to isoproterenol, indicating that the cell-permeable peptides did not affect short-term desensitization (Fig. 1*C*). To determine the effect of these peptides on resensitization, the cells were exposed to isoproterenol, in the presence of the peptides, for 3 h to desensitize and internalize the WT β_1-AR. Then the agonist was removed, and 10

μM alprenolol and 10 μM of each peptide was added to initiate recycling of the β_1-AR for the next 1.5 h. In cells exposed to st-Ht31-*pro*, the β_1-AR recovered from desensitization such that isoproterenol-stimulated adenylyl cyclase activity was comparable with control "nondesensitized" cells (Fig. 1*C*). In contrast, following exposure to st-Ht31, the activation of adenylyl cyclase by the β_1-AR remained significantly reduced, indicative of persistently desensitized receptors (Fig. 1*C*). Thus, disruption of PKA·AKAP complexes interfered with functional resensitization of the β_1-AR, indicating that proper PKA anchoring is also essential for β_1-AR resensitization.

AKAP79 Is Involved in Recycling of the Agonist-internalized β_1-AR in HEK-293 Cells—The character of the individual AKAPs and PKA subunits that are expressed in HEK-293 cells is unknown. As a first step toward characterization of the AKAP involved in PKA-mediated resensitization of the β_1-AR in HEK-293 cells, the AKAPs that were most prominently expressed in this cell line were identified by RII overlay assays. Interaction of ^{32}P-labeled RIIα subunit of PKA and extracts prepared from HEK-293 cells identified three clusters that interacted with the RIIα subunit (Fig. 2*A*). These clusters migrated with a calculated molecular mass value (in kilodaltons) between 75 and 82, 145 and 155, and 240 and 260. To identify the specific AKAP corresponding to each cluster, extracts prepared from HEK-293 cells were probed with antibodies to AKAPs whose molecular weights were within the M_r ranges of each cluster. These immunoblots identified the faster migrating cluster as AKAP79, the cluster with the intermediate M_r as AKAP149, and the slowest migrating cluster as AKAP250 (gravin) (Fig. 2*B*). Using antibodies directed against the various PKA subunits, the 41-kDa catalytic α-subunit and the 48-kDa regulatory RIα, RIIα, and RIIβ subunits of PKA were detected in HEK-293 cells (data not shown).

We reasoned that if one of these AKAPs is functionally involved in recycling of the agonist internalized β_1-AR then its selective down-regulation would interfere with receptor recycling. A specific and effective method for down-regulating the expression of selected genes is RNA interference using short interfering double-stranded RNA (siRNA) (36). Therefore, we generated siRNAs against the membranous AKAPs, namely AKAP79 and gravin, and determined their effect on endogenous AKAP expression by Western blotting. In addition, we tested the effect of the AKAP79 siRNA on the fluorescence of transiently transfected GFP-AKAP79 into naïve HEK-293 cells (Fig. 2, *C* and *D*). The AKAP79 siRNA reduced the levels of AKAP79 or the fluorescence of GFP-AKAP79 by >85%, whereas the scrambled duplex siRNA had no such effect (Fig. 2, *C* and *D*). The gravin siRNA reduced gravin expression by >80% (data not shown).

The effects of these siRNAs on recycling of the agonist-internalized β_1-AR were determined by confocal recycling assays (1). HEK-293 cells stably expressing the FLAG-tagged β_1-AR were transiently transfected with 100 nM control or active siRNA for 2 days. We determined by [^{3}H]CGP-12177 binding that these siRNAs did not affect the density of cell surface β_1-AR or had an appreciable effect on basal adenylyl cyclase activity (data not shown). Isoproterenol induced the internalization of the β_1-AR, and the rate and magnitude of its sequestration were not affected by any of the siRNAs. The confocal recycling assay indicated that the scrambled siRNA did not interfere with recycling of the WT β_1-AR, which was re-inserted into the membrane within 1 h after the removal of isoproterenol (Fig. 2*E*, *panels a–c*). In contrast, AKAP79 siRNA prevented the recycling of the agonist-internalized WT β_1-AR, as indexed by the cytoplasmic distribution of β_1-AR fluorescence after 1 h from initiating the recycling of the β_1-AR (Fig. 2*E*, *panels d–f*). Importantly, siRNA directed against gravin did not interfere with the recycling of agonist-internalized β_1-AR, which recycled quickly and efficiently (Fig. 2*E*, *panels g–i*). Therefore, endogenous AKAP79 selectively contributes to β_1-AR recycling.

Characterization of the Association between the β_1-AR, AKAP79, and PKA by Co-immunoprecipitations and Pulldown Assays—In cells stably expressing FLAG-AKAP79 and Myc-β_1-AR, antibodies against the FLAG tag co-immunoprecipitated the β_1-AR (Fig. 3*A*), suggesting that β_1-AR interacts with AKAP79. This is further supported by the reciprocal co-immunoprecipitation of YFP-AKAP79 with β_1-AR in cells co-expressing FLAG-β_1-AR and YFP-AKAP79 (Fig. 3*B*). In contrast, immunoprecipitation of FLAG-β_1-AR did not co-immunoprecipitate gravin, indicating that gravin did not associate with the β_1-AR under these conditions (Fig. 3*C*). This suggests that β_1-AR selectively interacts with AKAP79. Importantly, in cells co-expressing FLAG-β_1-AR and YFP-AKAP79, antibodies directed against the FLAG tag co-immunoprecipitated the RIIα and anti-RIIβ subunits of PKA (Fig. 3, *D* and *E*). Thus, AKAP79 and PKA were associated with β_1-AR in HEK-293 cells.

The association between AKAP79 and β_1-AR was explored in cells that endogenously express the β_1-AR and AKAP79 such as human neuroepithelioma SK-N-MC cells and neonatal rat cortical neurons (37, 38). Immunoprecipitation of AKAP79 from SK-N-MC cells co-immunoprecipitated the β_1-AR and reciprocal immunoprecipitations of β_1-AR co-immunoprecipitated AKAP79 (Fig. 4*A*). The homologue of AKAP79 expressed in the rat is AKAP150 (39). Immunoprecipitation of the β_1-AR from rat brain or neonatal rat cortical neurons co-immunoprecipitated AKAP150 and reciprocal immunoprecipitations of AKAP150 from rat brain co-immunoprecipitated the β_1-AR, indicating that the association between β_1-AR and AKAP79/150 occurred also in neurons (Fig. 4, *B* and *C*).

The involvement of AKAP-PKA interactions in recycling the agonist-internalized β_1-AR in SK-N-MC or neonatal rat cortical neurons was verified by recycling assays of biotinylated receptors (Fig. 4*D*). In these assays, neuronal cells were pre-exposed to st-Ht31 to disrupt PKA-AKAP interactions or to its inactive counterpart st-Ht31-*pro*. Then the cells were surface biotinylated with cleavable biotin followed by quenching of excess biotin with glycine. The amount of biotin incorporated into β_1-AR under this condition indexes total cellular β_1-AR biotinylation (Fig. 4*D*, *lanes 1* and *6*). The cells were then exposed to isoproterenol for 30 min, followed by cleavage of the remaining cell surface biotin (Fig. 4*D*, *lanes 2* and *7*). The amount of biotin recovered in this step indexes the amount of biotinylated β_1-AR that were internalized in response to isoproterenol. Thus, the ratio of internal biotin to total biotin incorporated into the β_1-AR indexes the percentile of surface

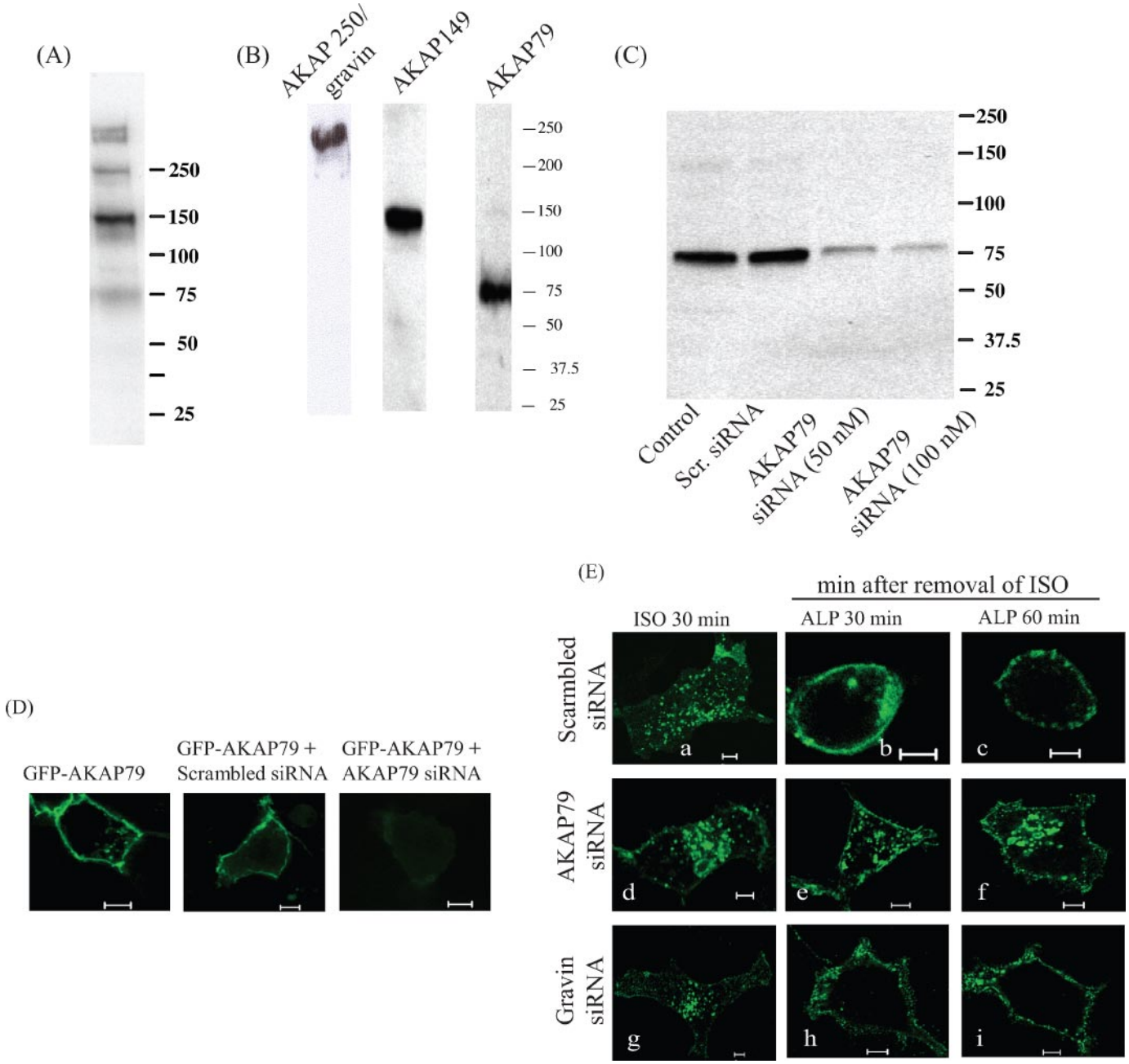

FIGURE 2. **Characterization of AKAP in HEK-293 cells and their role on recycling of the agonist-internalized β_1-AR.** *A*, HEK-293 cells extracts (25 μg/lane) were immunoblotted onto nitrocellulose filters and then hybridized to the ^{32}P-labeled RIIα subunit of PKA. The interacting proteins were identified by autoradiography. *B*, immunoblots of HEK-293 cell extracts (15 μg/lane) were probed with several anti-AKAP antibodies to identify the specific AKAPs expressed in these cells. *C*, HEK-293 cells were transiently transfected as follows: *first lane*, untreated cells; *second lane*, 100 nM scrambled siRNA; *third* and *fourth lanes*, 50 and 100 nM AKAP79 siRNA, respectively. After 2 days, cell extracts were probed for AKAP79 expression by Western blotting. *D*, HEK-293 cells expressing GFP-tagged AKAP79 were transfected with scrambled or AKAP79 siRNA for 2 days and the fluorescence in these cells was compared by confocal microscopy. *E*, HEK-293 cells were transfected with FLAG-tagged WT β_1-AR and with 100 nM of the indicated siRNA. After 2 days the cells were labeled with fluorescein isothiocyanate anti-FLAG antibody and recycling was conducted as described in the legend of Fig. 1.

β_1-AR that was internalized in response to isoproterenol. The data in Fig. 4*D* indicate that the Ht31 peptides did not markedly affect internalization of the β_1-AR in either cell type. To determine the effect of PKA-AKAP interactions on recycling of the agonist-internalized β_1-AR, isoproterenol was replaced with the β-antagonist alprenolol to inhibit β_1-AR internalization. Then the internalized β_1-AR was allowed to recycle by warming the cells (at 37 °C) for an additional 15, 30, or 60 min (Fig. 4*D*, *lanes 3–5* and *8–10*). After each time period, the cells were cooled to 4 °C and cleaved for the second time to ensure cleavage of any newly appearing surface biotin. Thus, the loss of biotin from the second cleavage step indexed recycling of the β_1-AR. The data reveal that by 60 min more than 90% of the biotin was lost from β_1-AR in cells pre-exposed to st-Ht31-*pro*, reflecting membrane recycling of β_1-AR and subsequent biotin cleavage (Fig. 4*D*, *lanes 3–5*). In contrast, the internalized (bio-

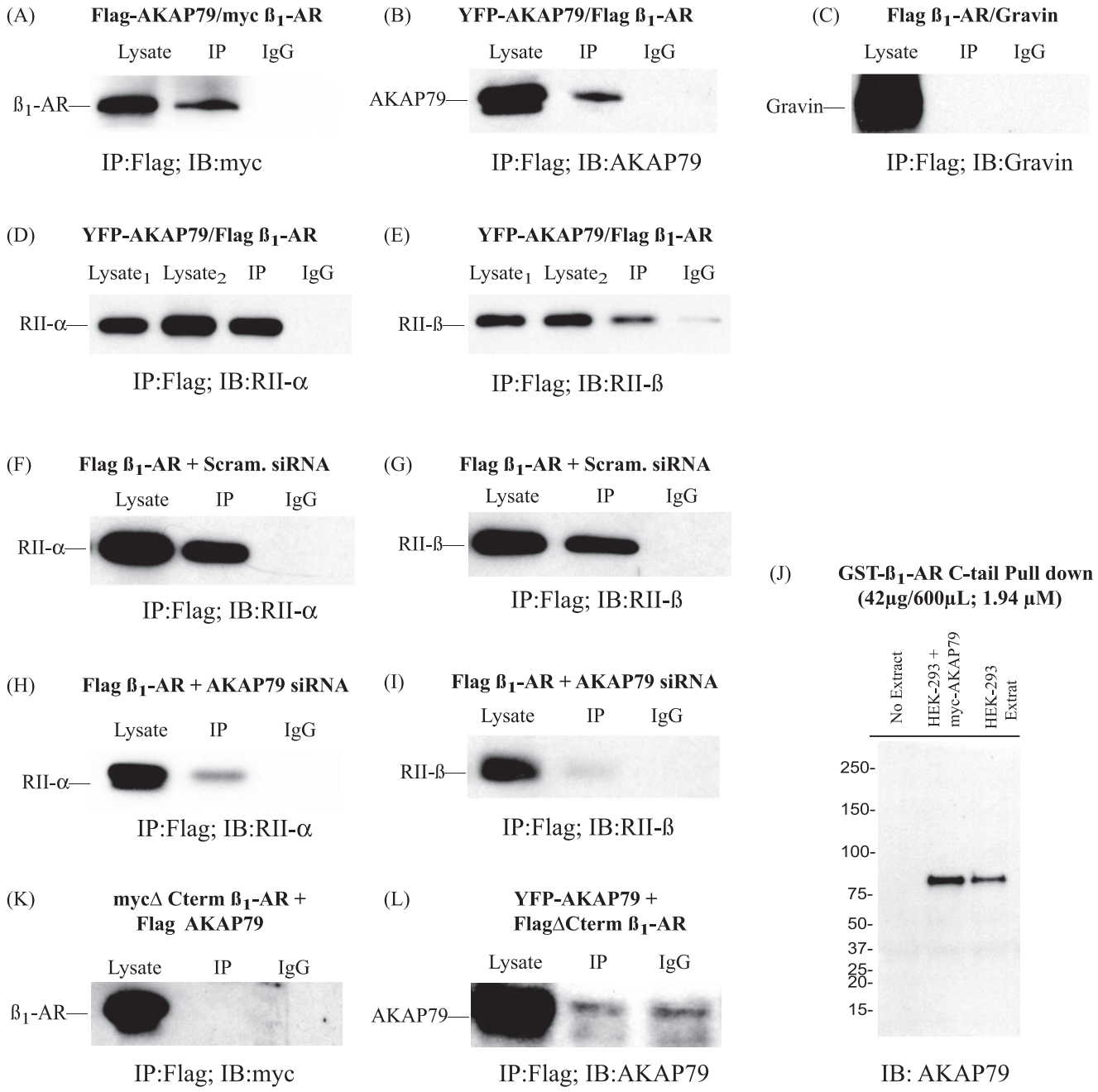

FIGURE 3. **Role of AKAP79 in the targeting of PKA to the β_1-AR microdomain: analysis by co-immunoprecipitation.** *A–C*, HEK-293 cells were co-transfected with the indicated constructs of AKAP79, gravin, and WT β_1-AR. In all experiments, equal amounts of lysates were incubated anti-tag IgG beads and with normal mouse IgG-conjugated to agarose beads to control for nonspecific antigen/antibody interactions. The immunoprecipitates were resolved on SDS-PAGE, blotted, and probed with the indicated antibodies. Lysates represent 2% of the total extract; whereas immunoprecipitations represent 30% of the total volume. *D* and *E*, HEK-293 cells stably expressing YFK-AKAP79 were co-transfected with FLAG-WT β_1-AR for 2 days. In all experiments, equal amounts of lysates from untransfected cells (*lysate$_1$*) or cells that were transfected with the β_1-AR (*lysate$_2$*) were incubated anti-tag IgG beads and with normal mouse IgG-conjugated to agarose beads to control for nonspecific antigen-antibody interactions. *F–I*, HEK-293 cells stably expressing the FLAG-WT β_1-AR were transiently transfected with 100 nM scrambled siRNA or AKAP79 siRNA for 2 days followed by immunoprecipitation and blotting as indicated. *J–L*, HEK-293 cells were transiently transfected with the epitope-tagged β_1-AR-(1–424) and AKAP79 for 2 days, followed by immunoprecipitation and blotting (*IB*) as indicated.

tinylated) β_1-AR in SK-N-MC or neonatal rat cortical neurons that were pretreated with st-Ht31 was not changed even after 1 h from the removal of isoproterenol, reflecting their internal distribution (Fig. 4*D*, compare *lanes 9* and *10* with *lanes 4* and *5*). These data indicate that AKAP/PKA interactions were also required for recycling of the endogenous β_1-AR in neurons.

To verify whether AKAP79 is involved in targeting PKA to the β_1-AR, HEK-293 cells stably expressing FLAG-β_1-AR were treated with AKAP79 siRNA or with its scrambled control (Fig. 3, *F–I*). RIIα and RIIβ subunits were effectively co-immunoprecipitated with β_1-AR in cells treated with control siRNA (Fig. 3, *F* and *G*). However, siRNA mediated suppression of AKAP79 markedly reduced the amounts of RIIα and RIIβ subunits co-

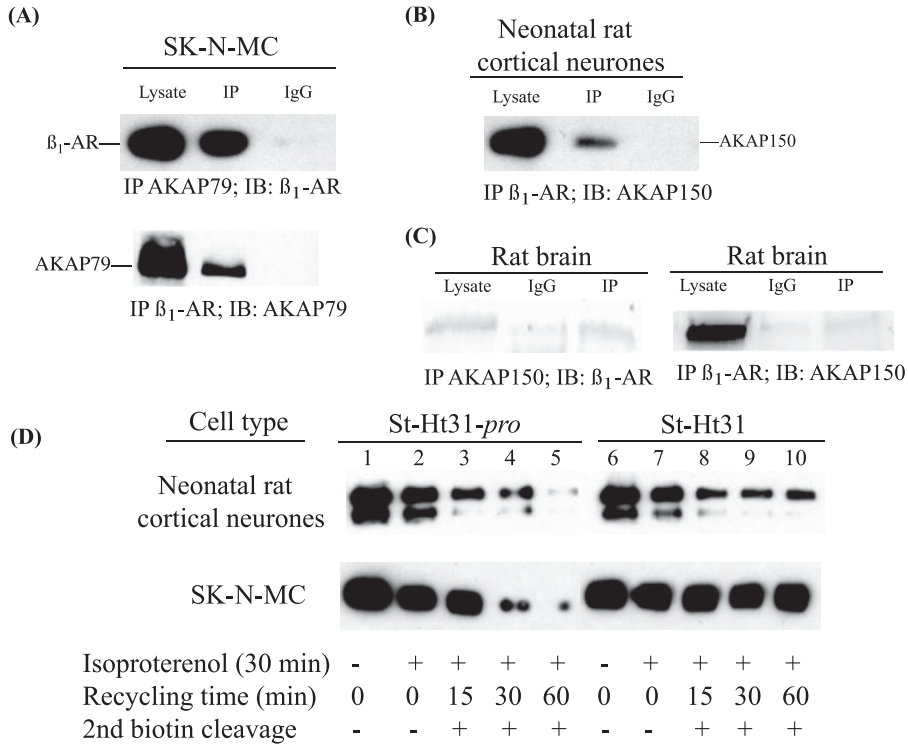

FIGURE 4. **Role of AKAP-PKA interactions in recycling of the β_1-AR in neuronal cells.** *A* and *B*, cell lysates from human neuroepithelioma SK-N-MC or rat neonatal cortical neurons were incubated with the indicated antibody for 16 h at 4 °C. Then 50 μl of protein G-agarose beads were added for an additional 2 h at 4 °C, followed by immunoprecipitation and blotting as indicated. *C*, rat whole brain lysates were incubated with 2 μg/ml of the indicated antibody and protein A/G-agarose beads for 16 h at 4 °C. Beads were washed 4 times and blotted with the indicated antibodies. *D*, several 10-cm culture dishes of SK-N-MC cells or rat neonatal cortical neurons in DMEM + 25 mM HEPES were incubated with 50 μM st-Ht31-*pro* (*lanes 1–5*) or st-Ht-31 (*lanes 6–10*) at 37 °C for 30 min. Then the cells were surface biotinylated and one set of plates was removed to determine total biotinylation for each cell line (*lanes 1* and *6*). The remaining sets of culture dishes were exposed to isoproterenol for 30 min at 37 °C to induce β_1-AR internalization, followed by removal of isoproterenol and cleavage of the remaining surface biotin (1st cleavage) with glutathione (*lanes 2–5* and *7–10*). One set of plates was extracted to determine the amount of internalized biotinylated β_1-AR (*lanes 2* and *7*). The remaining cultures were switched to warm culture medium supplemented with 10 μM β-adrenergic receptor antagonist alprenolol and 20 μM of either st-Ht31-*pro* or st-Ht31, then returned to 37 °C to allow the internalized β_1-AR to recycle for 15, 30, and 60 min. After each time period, the cells were recleaved (2nd cleavage) to ensure cleavage of any newly appearing (recycled) surface biotin. After the second cleavage, the cells were solubilized in RIPA buffer, and equal amounts of protein were mixed with 50 μl of bovine serum albumin-blocked ultralink-neutra avidin beads at 4 °C overnight. After washing the resin, the proteins were extracted with 2× Laemmli sample buffer, electrophoresed, and then electroblotted to nitrocellulose. The filters were probed with 1:250 dilution of the anti-β_1-AR antibody and visualized with horseradish peroxidase-conjugated donkey anti-rabbit IgG.

immunoprecipitated with the β_1-AR (Fig. 3, *H* and *I*). Collectively, these results indicate that endogenous AKAP79 is required for targeting PKA to the β_1-AR.

Most of the binding sites for β_1-AR-interacting proteins are contained within the 3rd IC and the carboxyl-terminal tail of the receptor (40, 41). As a first step toward determining the locus for association between β_1-AR and AKAP79, the carboxyl-terminal 53 amino acids between 425 and 477 in the β_1-AR were fused to GST and bacterial lysates were purified by affinity chromatography. HEK-293 cells transiently expressing pcDNA 3.1 or AKAP79 in pcDNA 3.1 were lysed and subjected to pull down using GST-β_1-AR-(425–477) as bait. As shown in Fig. 3*J*, GST-β_1-AR-(425–477) could pull down AKAP79 from control and AKAP79 expressing cells. In follow up experiments, cells expressing AKAP79 were transfected with the carboxyl-terminal truncated β_1-AR (β_1-AR-(1–424)), in which the last 53 amino acids in the carboxyl tail were deleted and subjected to immunoprecipitation. Reciprocal immunoprecipitation of either β_1-AR-(1–424) or AKAP79 did not lead to effective association of the AKAP or β_1-AR, respectively, as was previously observed for the full-length WT β_1-AR (Fig. 3, *K* and *L*). Therefore, it appears that the carboxyl-terminal tail of the β_1-AR harbors the principal determinants for AKAP79 association.

Characterization of the Association between the β_1-AR, AKAP79, and PKA by FRET Microscopy—Confocal video microscopy confirmed the membranous distribution of AKAP79 in HEK-293 cells (Fig. 5*A*). To determine whether AKAP79 and β_1-AR were colocalized, GFP-AKAP79 was expressed with FLAG-β_1-AR and their distribution was determined by dual-labeling confocal microscopy. GFP-AKAP79 (*green*) co-localized with the Cy3-labeled β_1-AR (*red*), as indexed by their combined yellow fluorescence (Fig. 5*B*). Exposing these cells to isoproterenol caused selective internalization of the β_1-AR, without altering the membranous distribution of AKAP79. Within 45 min after the initiation of recycling, the β_1-AR trafficked back into the cell membrane and were co-localized with AKAP79. These data show that colocalization between AKAP79 and β_1-AR is reversible and that AKAP79 is not appreciably internalized.

FRET microscopy was used to supplement the data obtained by immunoprecipitation and determine the relative strength of protein/protein interactions between the β_1-AR, AKAP79, and PKA. FRET relies on the transfer of energy from an excited donor (CFP) to an acceptor (YFP) if the two-tagged proteins are in very close proximity (<50Å) (22). Prior to the initiation of FRET, the localization, internalization, and recycling of β_1-AR-YFP- or -CFP chimera in HEK-293 cells were determined by confocal microscopy (Fig. 5*C*). These experiments show that the β_1-AR-YFP is expressed in the membrane, and that the receptor is internalized in response to isoproterenol (Fig. 5*C*, *panels a* and *b*). Removal of isoproterenol caused rapid recycling of β_1-AR-YFP with kinetics similar to those of the WT β_1-AR (Fig. 5*C*, *panels c–f*).

To determine the magnitude of FRET between the β_1-AR and AKAP79, the WT β_1-AR-CFP and AKAP79-YFP were transiently transfected into HEK-293 and imaged in live cells

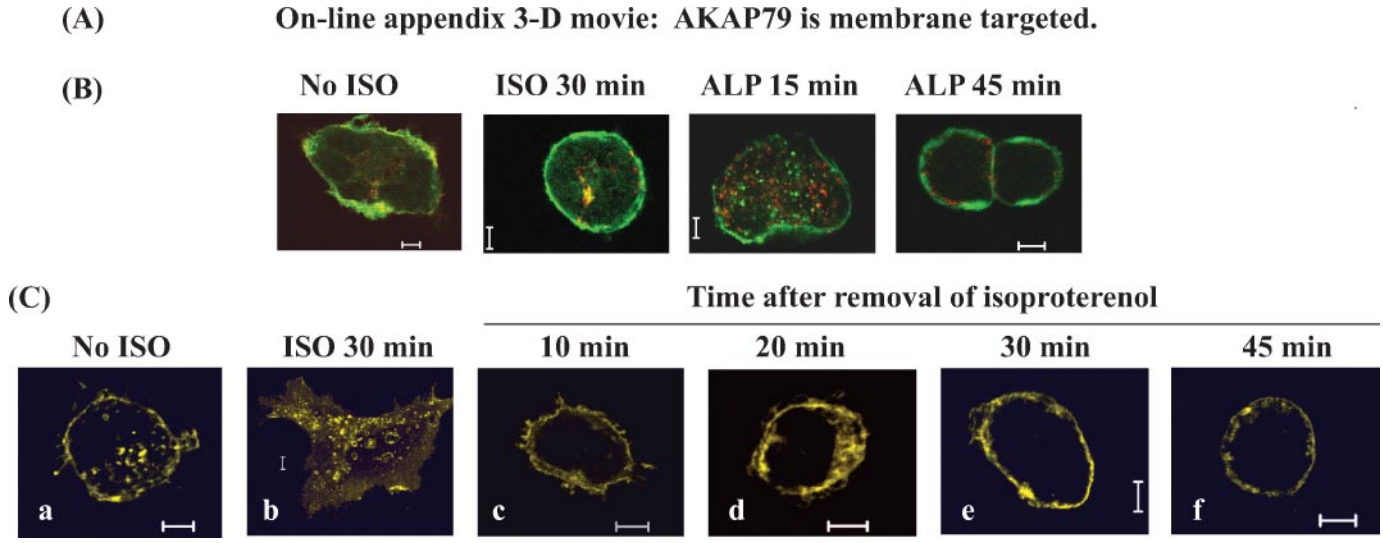

FIGURE 5. **The wild-type β_1-AR colocalizes with AKAP79 on the membrane.** *A*, AKAP79 is membrane-targeted protein (supplemental movie 1). *B*, a stable cell line of FLAG-tagged WT β_1-AR was transfected with GFP-AKAP79. Two days later, the cells were labeled with Cy3 anti-FLAG antibody to label the β_1-AR. The cells were exposed to 10 μM isoproterenol (*ISO*) for 30 min, acid washed, and treated with 100 μM alprenolol for 30 min and 1 h. Dual confocal images of AKAP79 (*green*) and β_1-AR (*red*) were taken at each time point. *C*, cells expressing WT β_1-AR-YFP were exposed to 10 μM isoproterenol for 20 min to internalize the β_1-AR, then the recycling of the receptor was visualized by confocal microscopy as described in the legend of Fig. 1.

on glass bottom dishes (Fig. 6*B*). The FRET*N* technique as measured by the sensitized emission method (27) was used to determine the binding of the β_1-AR to AKAP79 and to the RII subunit in live cells. This method generates high-resolution, real-time images of sensitized emission FRET using image subtraction, which allows comparison of FRET from multiple cells for a given acceptor-donor pair to demonstrate data reproducibility (Table 1 and "Experimental Procedures"). The FRET*N* revealed association between the β_1-AR and AKAP79 (Fig. 6*A*) with FRET efficiency of 12 ± 1.1%, suggesting that AKAP79 interacted with moderate affinity with the WT β_1-AR. In cells expressing AKAP79-CFP and AKAP79-YFP, significant colocalization was observed (Fig. 6*A*) but no FRET*N* was detected, suggesting that AKAP79 did not dimerize under these conditions.

One of the main functions of AKAP79 is to organize individual signaling molecules such as PKA into connected networks (18, 20, 42). FRET imaging of the interaction between AKAP79 and the RII subunit of PKA in Fig. 6*B* revealed a 17 ± 5.0% FRET*N*, in agreement with previously published data (22). By virtue of the association between PKA with AKAP79, and between AKAP79 and the β_1-AR, we would expect AKAP79 to target PKA to its potential substrate, the β_1-AR. To test this hypothesis, FRET*N* in cells expressing WT β_1-AR-YFP and RIIα-CFP were determined (Fig. 6*C*). The imaging data indicated that FRET*N* between these molecules was 22 ± 3.0%, suggesting that the RIIα subunit interacted with the β_1-AR with high affinity. In contrast the ability of the RIIα subunit to interact with the β_1-AR was ablated following treatment with AKAP79 siRNA. Therefore the human β_1-AR interacted with AKAP79 and the RII subunit of PKA (Fig. 6*D*).

To confirm FRET*N* measurements, the FRET experiments were repeated using the acceptor photobleaching method to determine FRET efficiencies in fixed cells (Fig. 7 and Table 1). FRET efficiencies (%) were very reproducible across several experiments (n = 8) for AKAP79-CFP and WT β_1-AR-YFP (8 ± 2.0%), and for AKAP79-YFP paired with RII-CFP (17 ± 1.2%) (Table 1). FRET data that were obtained by two different methods demonstrated that direct interactions between the β_1-AR, AKAP79, and the RII subunit of PKA occurred in live and fixed HEK-293 cells.

Role AKAP79-PKA Interactions in Agonist-mediated Phosphorylation of the β_1-AR—The activation of the β_1-AR signaling pathway by isoproterenol is associated with the generation of cyclic AMP that binds to the R subunit of PKA and releases the C subunit to phosphorylate target proteins. Inhibition of PKA or mutagenesis of its putative substrate Ser^{312} to alanine in the 3rd IC (S312A) prevented the recycling and resensitization of the β_1-AR (1). AKAP79 is also involved in recycling and resensitization of the β_1-AR, but its mechanism of action is not known. A potential mechanism that might be involved is that the targeting of PKA to the β_1-AR by AKAP79 is required for the phosphorylation of the β_1-AR by PKA. Therefore, we determined if PKA phosphorylates the β_1-AR and if AKAP79 was required.

The phosphorylation of the WT β_1-AR was markedly increased (6 ± 1-fold) upon exposing the cells to isoproterenol (Fig. 8*A*). Agonist-mediated phosphorylation of the β_1-AR is mediated by GRK and PKA (5). The preferred substrates for phosphorylation by PKA are serine/threonine residues that are preceded by R*X*- or RR*X*- (where *X* is any amino acid and R is arginine), whereas the preferred substrates for phosphorylation by GRK are serine/threonine residues that are preceded by an acidic amino acid (43–46). The sequence around Ser^{312} in the 3rd IC is RRPS^{312}, which is a preferred site for phosphorylation by PKA (1, 43), whereas serines/threonines that are preceded by an acidic amino acid reside exclusively in the carboxyl-terminal tail of the β_1-AR (45). Inhibition of PKA by myristoylated PKI (mPKI), a cell-permeable specific PKA inhibitor (47), reduced the phosphorylation of the WT β_1-AR by 30 ± 6% (n = 3). These data indicate that the PKA component accounted for ~25% of total receptor phosphorylation, which agrees with the

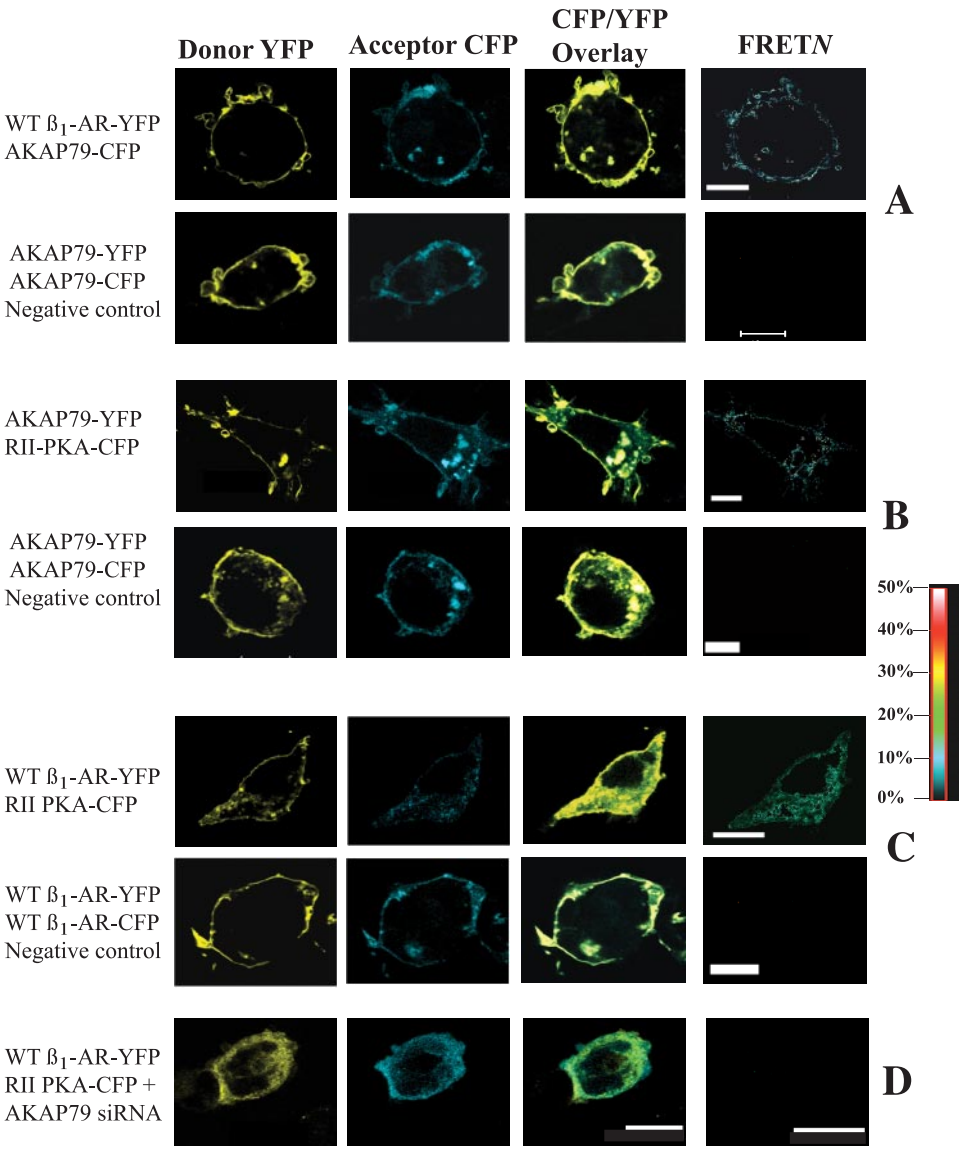

FIGURE 6. **Sensitized emission FRET microscopy between AKAP79, WT β_1-AR, and the PKA RIIα subunit.** *A*, cells co-expressing the WT β_1-AR-YFP and AKAP79-CFP were used. *B*, live cells, expressing AKAP79-YFP and RII-CFP were imaged at room temperature in glass-bottom Petri dishes. *C*, direct binding of PKA RIIα-CFP to WT β_1-AR-YFP. *D*, FRET between PKA RII-CFP and the WT β1-AR-YFP was not observed in HEK-293 cells when AKAP79 was knocked down with siRNA. Negative controls were performed with AKAP79 (*A* and *B*) and WT β_1-AR (*C*), labeled with both fluorescent tags. FRET*N* is present in pseudocolor. Normalized FRET*N* values were calculated using LSM510 Macro 1.5 FRET software using Equation 1 as described under "Experimental Procedures." FRET*N* values for the various constructs are presented in Table 1.

TABLE 1

Normalized FRET efficiencies in % as recorded by the sensitized emission method (FRET*N*) in live cells or by the acceptor photobleaching method in fixed cells

FRET efficiency was calculated using area averages for donor (D) before and after bleaching. FRET = (D after − D before)/D after. Donor (D) and acceptor (A) threshold values were subtracted from all pixels before FRET calculation. The mean values of FRET efficiencies calculated for at least 10 specific regions of interest in each FRET pair from seven experiments were collected and analyzed with FRET tool software for LSM510 version 3.2.

CFP donor	YFP acceptor			
	FRET*N*		Acceptor photobleaching	
	β_1-AR	AKAP79	β_1-AR	AKAP79
RII-PKA	22 ± 3	17 ± 5	17 ± 1.2	15 ± 9
AKAP79	12 ± 1.1	No FRET	8 ± 2.0	No FRET
β_1-AR	No FRET	10 ± 2	No FRET	10 ± 1.9

stoichiometry of GRK *versus* PKA phosphorylatable serines in the human β_1-AR.

To determine whether Ser^{312} is a potential substrate for phosphorylation by PKA, the phosphorylation of S312A in response to isoproterenol was determined. The phosphorylation of S312A increased by ~5-fold in response to isoproterenol. mPKI did not reduce the phosphorylation of S312A, suggesting that Ser^{312} was a potential substrate for PKA (Fig. 8*A*).

To provide stronger evidence that Ser^{312} was potentially phosphorylated by PKA, the WT β_1-AR and S312A were phosphorylated in response to isoproterenol followed by cleavage of each ^{32}P-labeled receptor with cyanogen bromide (33, 34). The human β_1-AR is cleaved at methionine residues by cyanogen bromide into peptides that are 4, 9, 33, 44, 69, 91, and 147 amino acids in length. Of these, the 91-amino acid peptide (between amino acids 240 and 330) contains the entire third intracellular loop and the 147-amino acid peptide (between 331 and 477) contains the entire carboxyl-terminal tail. Cyanogen bromide cleavage of the ^{32}P-labeled WT β_1-AR isolated from cells that were exposed to isoproterenol generated two phosphopeptides of molecular mass = 10 and 15 kDa (Fig. 8*B*). The size of the 10-kDa peptide corresponds to the expected molecular mass of the 3rd IC-derived phosphopeptide and the 15-kDa peptide corresponded to the expected molecular mass of the carboxyl terminus-derived phosphopeptide. The % of the total cpm of ^{32}P incorporated into the 10-kDa band derived from the WT β_1-AR was 27 ± 5%, which is in agreement with the mPKI data in Fig. 7*A*. Cleavage of the phosphorylated S312A with cyanogen bromide indicated that 94 ± 6% of the ^{32}P was incorporated into the 15-kDa peptide and ~6 ± 3% was incorporated into the 10-kDa peptide.

Pretreatment of cells expressing the WT β_1-AR with mPKI reduced the phosphorylation of the 10-kDa peptide from 30% to ~7%, in agreement with the assumption that this peptide contained the putative PKA-phosphorylated serine in the 3rd IC. The percentage of the total cpm incorporated into the 10-kDa peptide derived from mPKI-treated S312A was ~7% also. Thus, the percentage of ^{32}P incorporated into the 10-kDa peptide derived from

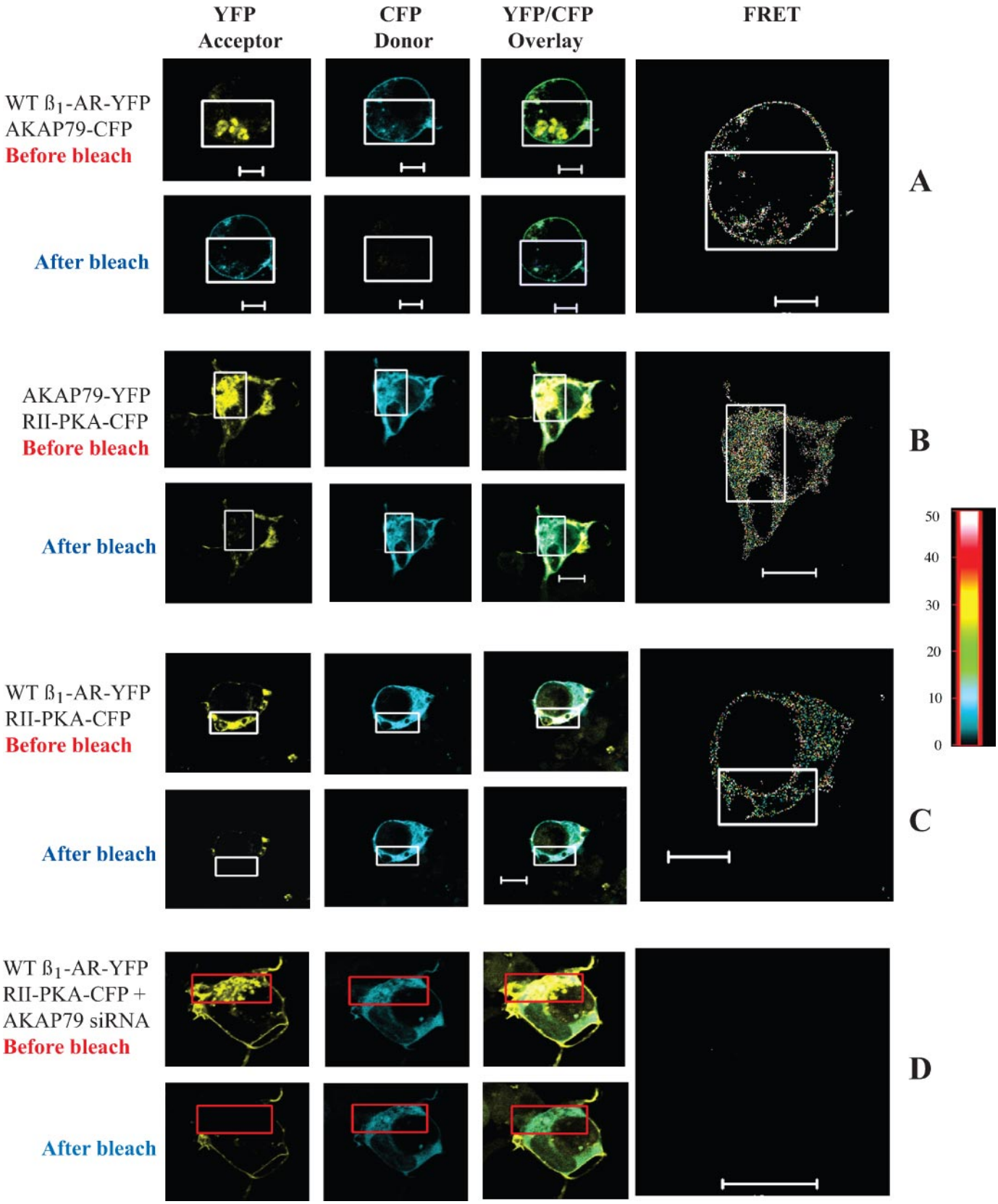

FIGURE 7. **Acceptor photobleaching analysis of FRET interactions between AKAP79, WT β_1-AR, and the PKA RIIα subunit.** By observing donor (CFP) channel intensity changes upon bleaching of the acceptor (YFP), we obtained an image set consisting of a time lapse recording of donor and acceptor channels with acceptor photobleaching carried out in between. FRET was recorded by examining the quenching of CFP during acceptor (YFP) photobleaching by the 514-nm argon laser line. Lambda stacks were acquired at various time points before and after photobleaching of YFP. Upon acceptor (YFP) photobleaching, donor (CFP) intensity increased significantly (compare donor before bleach and merged images after bleach). The *color ruler* shows the relationship between the pseudo FRET color and the corresponding FRET efficiency reported in Table 1.

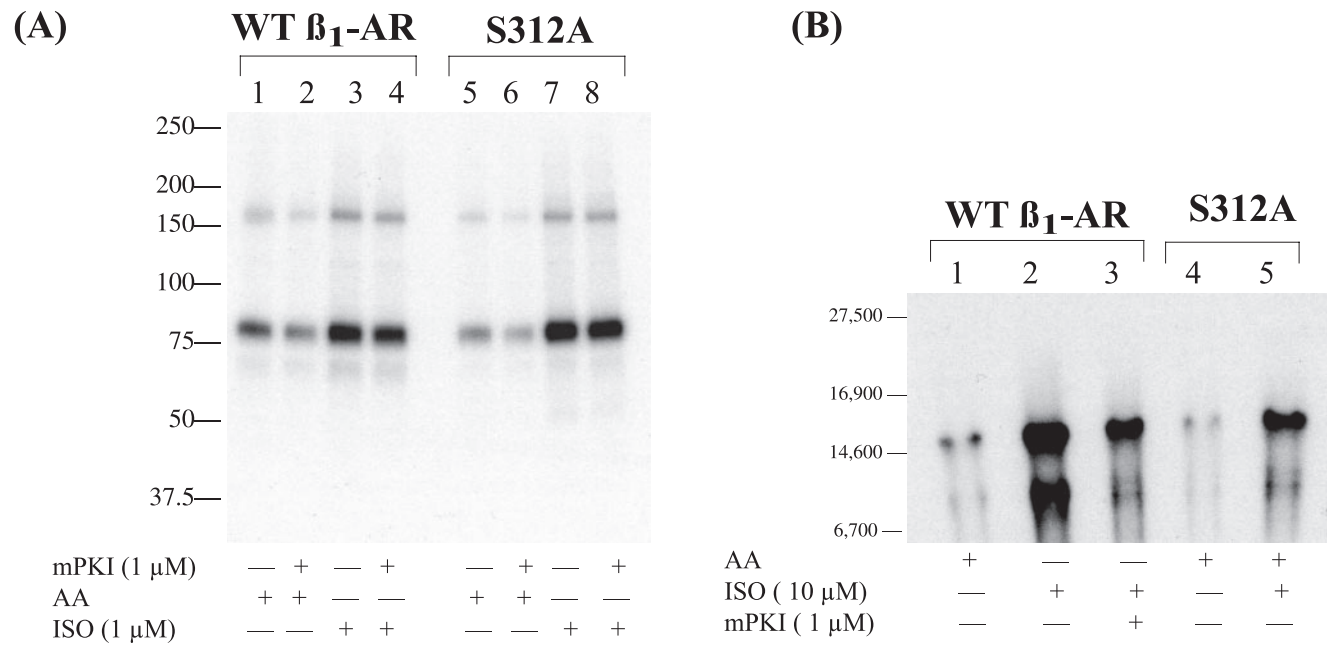

FIGURE 8. **Effect of inhibiting PKA on isoproterenol-mediated phosphorylation of the β_1-AR.** *A*, cells expressing the FLAG-tagged WT β_1-AR (*lanes 1–4*) or the Flag-tagged S312A (*lanes 5–8*) were metabolically labeled with $^{32}PO_4$, then incubated where indicated with 1 μM of myristoylated PKI for 30 min (*lanes 2, 4, 6,* and *8*). The cells were exposed to buffer (ascorbic acid 1% (*AA*)) (*lanes 1, 2, 5,* and *6*) or 10 μM isoproterenol for 10 min (*lanes 3, 4, 7,* and *8*). The β_1-AR was immunoprecipitated using anti-Flag IgG-agarose and subjected to SDS-PAGE and autoradiography. *B*, the immunoprecipitated β_1-AR were subjected to SDS-PAGE, followed by electroblotting to nitrocellulose. The bands corresponding to the ^{32}P-labeled β_1-AR were cut out and incubated with 100 μg/ml $CNBr^-$ in 70% formic acid for 1.5 h. The lyophilized peptides were electrophoresed on 16% Tricine-SDS gels. The gels were exposed to x-ray film for 1 day to generate the image in the figure and then counted electronically. In *lane 2*, the % cpm in the 10- *versus* the 15-kDa band were 30.7% (3,108 to 10,104 cpm, respectively). In *lane 3*, the % cpm in the 10- *versus* the 15-kDa band were 8% (253 to 3,282, respectively). In *lane 5*, the % cpm in the 10- *versus* the 15-kDa band were 8% (236 to 2,821 cpm, respectively). The cpm in *lanes 1* and *4* could not be accurately determined.

S312A was ~7% in the absence or presence of mPKI, whereas mPKI reduced the percentage of ^{32}P incorporated into the WT β_1-AR from 27 to 7%. Therefore, phosphorylation of the 3rd IC in the WT β_1-AR in mPKI-treated cells was similar to the phosphorylation of the 3rd IC in the S312A mutant in untreated cells.

The next series of experiments were designed to determine whether AKAP/PKA interactions or AKAP79 are involved in the PKA component of isoproterenol-mediated phosphorylation of the WT β_1-AR (Fig. 9*A*). HEK-293 cells were transiently transfected with the FLAG-tagged β_1-AR along with either scrambled control or AKAP79 siRNA. These, and cells expressing the FLAG-WT β_1-AR were metabolically labeled with 200 μCi of $^{32}PO_4$ for 1.5 h. Cells stably expressing the FLAG-β_1-AR were exposed for 45 min to 50 μM of either st-Ht31 or st-Ht31-*pro*. Then all the cells were exposed to 10 μM isoproterenol or buffer for 10 min followed by immunoprecipitation of the β_1-AR. Isoproterenol increased the phosphorylation of the WT β_1-AR in cells pretreated with st-Ht31-*pro* or the scrambled siRNA by 8 ± 2-fold. In those cells that were pretreated with st-Ht31 or the AKAP79 siRNA the corresponding increase in the phosphorylation of the WT β_1-AR was 5.6 ± 1-fold. Therefore, pretreatment with either st-Ht31 or AKAP79 siRNA reduced isoproterenol-mediated phosphorylation of the WT β_1-AR by ~30 ± 6%.

Cyanogen bromide cleavage of the phosphorylated WT β_1-AR derived from cells pretreated with either st-Ht31-*pro* or with the scrambled siRNA generated the 15- and 10-kDa phosphopeptides at a ~3:1 ratio (Fig. 9*B*, *lanes 1*, *2*, *5*, and *6*). On the other hand, cyanogen bromide cleavage of the β_1-AR derived from cells pretreated with either st-Ht31 or with the AKAP79 siRNA generated the 15-kDa phosphopeptide only (Fig. 9*B*, *lanes 3*, *4*, *7*, and *8*). Therefore, inhibition of AKAP-PKA interactions with st-Ht31 or with AKAP79 siRNA both inhibited the phosphorylation of the peptide derived from the 3rd IC, which contains the putative PKA substrate. These reagents also prevented the recycling of the agonist-internalized β_1-AR, indicating that AKAP79-anchored PKA was involved in resensitization of the β_1-AR and its signaling pathway.

DISCUSSION

Prolonged or repeated activation of many GPCRs induces rapid desensitization followed by a period during which the receptor is either resensitized or degraded (4, 7, 12). Desensitization of GPCR is a consequence of GRK-mediated phosphorylation of the agonist-occupied receptor and subsequent binding of β-arrestins, which together promote rapid desensitization and internalization of the GPCR (4–6). Resensitization refers to the phenomena that repopulate the plasma membrane with GPCRs and concomitantly restore signaling efficacy and specificity (7–9). For many GPCRs, it has been established that internalization is a prerequisite for resensitization as well as for degradation, but our understanding of the motifs in GPCRs, which impart these distinct outcomes, remains incomplete (8, 9).

To date, the best characterized motif controlling the fate of the internalized GPCR is the PDZ type 1 ligand in the COOH-terminal tail of the GPCR that when mutated inhibits recycling and resensitization of the GPCR (47–51). Recently, PKA and its substrate Ser^{312} in the 3rd IC of the human β_1-AR were found to

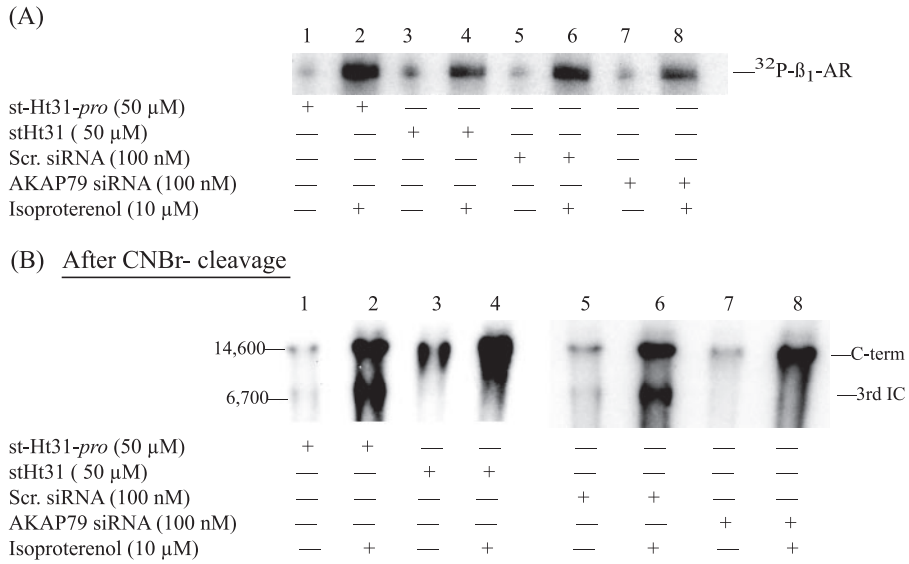

FIGURE 9. **Effect of st-Ht31 peptides and AKAP79 siRNAs on isoproterenol-mediated phosphorylation of the β_1-AR.** *A*, cells were transiently transfected with the FLAG-tagged WT β_1-AR and with either 100 nM scrambled siRNA or 100 nM AKAP79 siRNA. These cells were metabolically labeled with 200 μCi/ml of $^{32}PO_4$ for 1.5 h. In separate culture plates, cells that stably expressed the FLAG-tagged WT β_1-AR were metabolically labeled with 200 μCi/ml of $^{32}PO_4$ for 1.5 h. During the last 30 min of labeling, these cells were exposed to 50 μM st-Ht31 or st-Ht31-*pro*. Then all the cells were exposed to 1% ascorbic acid (*AA*) or 10 μM isoproterenol for 10 min as indicated. The β_1-AR was immunoprecipitated using anti-FLAG IgG-agarose and subjected to SDS-PAGE and autoradiography followed by electronic counting using the Instantimager™. *B*, the immunoprecipitated β_1-AR from all samples were cleaved with cyanogen bromide and electrophoresed on 16% Tricine-SDS gels. The gels were exposed to x-ray film for 1 day to generate the image in the figure and then counted electronically by the Instantimager.

be novel signals that are involved in recycling and resensitization of this GPCR (1).

The identification of PKA as a kinase involved in recycling of the human β_1-AR led us to seek potential intermediates that may target PKA to the β_1-AR. PKA is targeted to its numerous substrates by members of the AKAP family, which is composed of more than 70 members (18). Blockade of AKAP-PKA interactions with Ht31-derived peptides inhibited the recycling of exogenously and endogenously expressed β_1-AR, indicating that these interactions were required for recycling of the agonist-internalized β_1-AR (Figs. 1 and 4). Through the use of siRNA interference, a prominent role for AKAP79 in recycling of the β_1-AR was established. The involvement of AKAP79 in targeting PKA to the β_1-AR was further verified by co-immunoprecipitation, which revealed that an AKAP79·PKA complex was bound to the carboxyl terminus of the β_1-AR. This method, however, provides a relatively static view of the β_1-AR·AKAP79·PKA complex. A more dynamic view was provided by FRET microscopy that localized this ternary complex to the plasma membrane and indicated that the associations between β_1-AR and AKAP79/PKA occurred at relatively high efficiency. However, it must be emphasized that the strength of the FRET signal is a function of the distance between chromophores, the binding affinity of protein-protein interactions, and chromophore orientation within the complex (21, 25–28). Thus, differences between any of these parameters can affect the intensity of FRET signals between acceptor-donor pairs. For example, the weaker FRET signal that was measured between AKAP79/β_1-AR *versus* β_1-AR/RII was surprising because the data in *panels D* of Figs. 6 and 7 indicated that the formation of the β_1-AR·RII complex was mediated by AKAP79. These findings were corroborated in Fig. 3, which showed that the β_1-AR immunoprecipitants contained larger amounts of RII than AKAP79. We attribute these findings to different stoichiometries and chromophore separations between the β_1-AR and AKAP79 *versus* the β_1-AR and RII. For instance, whereas the PKA holoenzyme binds to AKAP79 with 1:1 stoichiometry, the tetrameric composition of PKA into two R and two C subunits generates a stoichiometry of 2:1 between the RII subunits and AKAP79. In this case, FRET between AKAP79 and β_1-AR involved a 1:1 stoichiometry, whereas that between the RII subunit and the β_1-AR involved a 2:1 stoichiometry if the interaction between RII and the β_1-AR was mediated by AKAP79. Thus, the weaker FRET signal between the β_1-AR and AKAP79 *versus* the β_1-AR and RII reflects an anticipated consequence of these stoichiometries and verifies that AKAP79 is the bridging molecule between the β_1-AR and RII dimer of PKA.

To provide a mechanistic foundation for the effect of AKAP79 on recycling of the β_1-AR we explored the role of AKAP79 and its associated scaffold on PKA-mediated phosphorylation of the β_1-AR. This is a particularly important question because Gardner *et al.* (1), have determined that PKA and its substrate Ser^{312} in the 3rd IC were involved in recycling and desensitization of the β_1-AR. However, to show that isoproterenol-mediated phosphorylation of the β_1-AR involves PKA is challenging because the distribution of PKA *versus* GRK phosphorylatable serines is ~1:3, respectively, whereas the standard error in phosphorylation experiments is typically between 8 and 12% (1, 34, 44–46). Thus, direct assessment of the PKA component was necessary to unambiguously analyze the effect of AKAP79 on this parameter. Using mPKI, we determined that the magnitude of the PKA component was ~25%, indicating that the expected stoichiometries of PKA- *versus* GRK-mediated phosphorylation of the β_1-AR were as expected. Cyanogen bromide cleavage of the phosphorylated β_1-AR confirmed that PKA-mediated phosphorylation of the β_1-AR was localized within the 3rd IC and that inhibition of PKA-AKAP interactions or down-regulation of AKAP79 inhibited this parameter, exclusively. We should point out, however, that even though the effect of mPKI was largely because of inhibition of PKA, a minor component was because of inhibition of GRK. As outlined in Fig. 8*A*, *lanes 2* and *6*, mPKI reduced basal phosphorylation of the WT β_1-AR and the PKA null β_1-AR S312A mutant, which we attribute to indirect inhibition of GRK by mPKI. Phosphorylation of GRK-2 by PKA at Ser^{685} enhances the translocation

of GRK-2 from the cytosol to the membrane where it phosphorylates the agonist-occupied β-AR (52). Thus, by inhibiting PKA we inadvertently reduced GRK-mediated phosphorylation of the carboxyl terminus of the β_1-AR, which was reflected by reduced ^{32}P incorporation in *lane 3* of Fig. 8*B*. The effects of st-Ht31 and AKAP79 siRNA on the phosphorylation of the β_1-AR were more pronounced than mPKI, illustrating the importance of AKAP79-mediated targeting of PKA in this phenomenon. These data are similar to the effect of st-Ht31 and the dominant negative AKAP79 (AKAP79-Pro) mutant on the phosphorylation of the β_2-AR in response to isoproterenol (53).

The characterization of the β_1-AR-AKAP79-PKA scaffold was determined by recycling assays that identified a novel function for AKAP79 as a mediator for the resensitization of this GPCR. This discovery increases the range of functions already attributed to AKAP79. AKAP79/β_2-AR interactions are important for facilitating the signaling and phosphorylation of the β_2-AR, as well as for regulating the cyclic AMP metabolism by an associated phosphodiesterase (19, 48). A prominent role for AKAP79/β_2-AR interactions was exerted on isoproterenol-mediated activation of mitogen-activated protein kinase, which was inhibited by the PKA inhibitor H-89, and by disrupting AKAP-PKA interactions with st-Ht31 or dominant negative AKAP79 (53). In the case of the β_1-AR, AKAP79 did not affect the magnitude of cyclic AMP accumulation, sequestration, or mitogen-activated protein kinase activation elicited by isoproterenol, rather it had a marked effect on its recycling and resensitization. The effects produced by PKA and AKAP79 on the β_1-AR were biologically similar, suggesting that AKAP79 exerted its effect on the β_1-AR largely by PKA-dependent mechanisms. The effects of PKA and AKAP79 on the β_2-AR, however, were not the same suggesting that AKAP79 exerted its effects on the β_2-AR by PKA-dependent (such as inhibition of mitogen-activated protein kinase) and independent (such as inhibition of the β_2-AR sequestration) mechanisms (54). The most plausible cause for the convergence of PKA- and AKAP79-dependent mechanisms in regulating the recycling of the β_1-AR is likely because both are integral to Ser^{312} phosphorylation.

AKAP250 (gravin) is another AKAP that interacted with the β_2-AR through its carboxyl-terminal tail (55). AKAP250 exerts numerous effects on the β_2-AR that include regulation of internalization, recycling, and recovery of the β_2-AR from agonist-induced desensitization (54–56). However, siRNA-mediated suppression of gravin in HEK-293 cells did not disrupt the recycling or the recovery of the β_1-AR from agonist-induced desensitization, indicating that the repertoire of AKAPs that bind to each GPCR promote distinct effects on these receptors.

The proposed AKAP79-PKA-targeting scaffold is a self-contained signalosome that might produce many effects other than recycling and resensitization of the β_1-AR. The diffusion of cyclic AMP generated by the activation of the β_1-AR signaling pathway is restricted by spatiotemporal mechanisms that limit its diffusion and reduce its half-life through degradation by phosphodiesterases, which are recruited by β-arrestins to the receptor microdomain (19). The identification of AKAP79 as a binding partner to the β_1-AR provides a potential mechanism to ensure faithful signal propagation from the β_1-AR to downstream targets that are also linked to AKAP79 such as the L-type Ca^{2+} channel and the GluR1 AMPA receptor subunit (21, 57).

Although we found that the carboxyl-terminal tail of the β_1-AR is necessary for AKAP79 association with the receptor, it remains to be determined whether this is through a direct or indirect interaction. In particular, the carboxyl terminus of the β_1-AR between amino acids 474 and 477 contains a PDZ type I ligand that binds to PSD-95, SAP97, as well as four other members of the membrane-associated guanylate kinase (MAGUK) family of scaffolding proteins (37, 57–61). AKAP79 is known to bind to the Src homology 3 and guanylate kinase-like domains of membrane-associated guanylate kinase proteins PSD-95 and SAP97 (62). Like AKAP79, SAP97 interacts with the GluR1 AMPA receptor subunit and the interaction between SAP97 and AKAP79 recruits PKA to ionotropic glutamate receptors (21, 62). Therefore, it is conceivable that multiplexing between a β_1-AR·MAGUK·AKAP79 complex might scaffold AMPA receptors and other signaling molecules to the β_1-AR microdomain to facilitate their heterologous phosphorylation by the β_1-AR signaling pathway as has been observed in hippocampal neurons (58). Therefore, the mélange of proteins scaffolded directly or indirectly to the β_1-AR or other GPCR produce the range responses that define the pharmacological character of individual GPCR.

Acknowledgments—We thank A. Naren, Associate Professor of Physiology at the University of Tennessee-HSC, for assistance with pull-down assays and Carolyn Mathews, the Confocal Microscopy Facility, for technical assistance.

REFERENCES

1. Gardner, L. A., Delos Santos, N. M., Matta, S. G., Whitt, M. A., and Bahouth, S. W. (2004) *J. Biol. Chem.* **279,** 21135–21143
2. Lohse, M. J., Engelhardt, S., and Eschenhagen, T. (2003) *Circ. Res.* **93,** 896–906
3. Xiao, R. P., Zhu, W., Zheng, M., Chakir, K., Bond, R., Lakatta, E. G., and Cheng, H. (2004) *Trends Pharmacol. Sci.* **25,** 358–365
4. Freedman, N. J., and Lefkowitz, R. J. (1996) *Recent Prog. Horm. Res.* **51,** 319–353
5. Lefkowitz, R. J. (1998) *J. Biol. Chem.* **273,** 18677–18680
6. Luttrell, L. M., Ferguson, S. S., Daaka, Y., Miller, W. E., Maudsley, S., Della Rocca, G. J., Lin, F., Kawakatsu, H., Owada, K., Luttrell, D. K., Caron, M. G., and Lefkowitz, R. J. (1999) *Science* **283,** 655–661
7. Yu, S. S., Lefkowitz, R. J., and Hausdorff, W. P. (1993) *J. Biol. Chem.* **268,** 337–341
8. Kreuger, K. M., Daaka, Y., Pitcher, J. A., and Lefkowitz, R. J. (1997) *J. Biol. Chem.* **272,** 5–8
9. Pipping, S., Andexinger, S., and Lohse, M. J. (1995) *Mol. Pharmacol.* **47,** 666–676
10. Whistler, J. L., Enquist, J., Marley, A., Fong, J., Gladher, F., Tsuruda, J., Murray, S. R., and von Zastrow, M. (2002) *Science* **297,** 615–620
11. Garland, A. M., Grady, E. F., Lovett, M., Vigna, S. R., Frucht, M. M., Krause, J. E., and Bunnett, N. W. (1996) *Mol. Pharmacol.* **49,** 438–446
12. Bremnes, T., Paasche, J. D., Mehlum, A., Sandberg, C., Bremnes, B., and Attramadal, H. (2000) *J. Biol. Chem.* **275,** 17596–17604
13. Seibert, F. S., Tabcharani, J. A., Chang, X. B., Dulhanty, A. M., Mathews, C., Hanrahan, J. W., and Riordan, J. R. (1995) *J. Biol. Chem.* **270,** 2158–2162
14. Katsura, T., Gustafson, C. E., Ausiello, D. A., and Brown, D. (1997) *Am. J. Physiol.* **272,** F817–F822
15. Ehlers, M. D. (2000) *Neuron* **28,** 511–525

16. Chrivia, J. C., Uhler, M. D., and McKnight, G. S. (1988) *J. Biol. Chem.* **263,** 5739–5744
17. Kim, C., Xuong, N. H., and Taylor, S. S. (2005) *Science* **301,** 690–696
18. Wong, W., and Scott, J. D. (2004) *Nat. Rev. Mol. Cell Biol.* **5,** 959–970
19. Lynch, M. J., Baillie, G. S., Mohamed, A., Li, X., Maisonneuve, C., Klussmann, E., van Heeke, G., and Houslay, M. D. (2005) *J. Biol. Chem.* **280,** 33178–33189
20. Klauck, T. M., Faux, M. C., Labudda, K., Langeberg, L. K., Jaken, S., and Scott, J. D. (1996) *Science* **271,** 1589–1592
21. Tavalin, S. J., Colledge, M., Hell, J. W., Langeberg, L. K., Huganir, R. L., and Scott, J. D. (2002) *J. Neurosci.* **22,** 3044–3051
22. Oliveria, S. F., Gomez, L. L., and Dell'Acqua, M. L. (2003) *J. Cell Biol.* **160,** 101–112
23. Snyder, E. M., Philpot, B. D., Huber, K. M., Dong, X., Fallon, J. R., and Bear, M. F. (2001) *Nat. Neurosci.* **4,** 1079–1085
24. Delos Santos, N. M., Gardner, L. A., White, S. B., and Bahouth, S. W. (2006) *J. Biol. Chem.* **281,** 12896–12907
25. Kenworthy, A. K. (2001) *Methods* (*Orlando*) **24,** 289–296
26. Sekar, R. B., and Periasamy, A. (2003) *J. Cell Biol.* **160,** 629–633
27. Gordon, G. W., Berry, G., Liang, X. H., Levin, B., and Herman B. (1998) *Biophys. J.* **74,** 2702–2713
28. Sorkin, A., McClure, F., Huang, G., and Carter, R. (2000) *Curr. Biol.* **10,** 1395–1398
29. Gu, Y., Di, W. L., Kelsell, D. P., and Zicha, D. (2004) *J. Microsc.* **215,** 162–173
30. Berney, C., and Danuser, G. (2003) *Biophys. J.* **84,** 3992–4010
31. Carr, D. W., Stofko-Hahn, R. E., Fraser, I. D. C., Bishop, S. M., Acott, T. S., Brennan, R. G., and Scott, J. D. (1991) *J. Biol. Chem.* **266,** 14188–14192
32. Bahouth, S. W. (1995) *Biochem. J.* **307,** 831–841
33. Luo, B., Hurley, T. R., and Sefton, B. M. (1991) *Methods Enzymol.* **201,** 149–156
34. Bahouth, S. W., Gokmen-Polar, Y., Coronel, E., and Fain, J. N. (1996) *Mol. Pharmacol.* **49,** 1049–1057
35. Vijayaraghavan, S., Goueli, S. A., Davey, M. P., and Carr, D. W. (1997) *J. Biol. Chem.* **272,** 4747–4752
36. Elbashir S. M., Harborth, J., Lendeckel, W., Yalcin, A., Weber, K., Tuschl, T. (2001) *Nature* **411,** 494–498
37. Hu, L. A., Tang, Y., Miller, W. E., Cong, M., Lau, A. G., Lekowitz, R. J., and Hall, R. A. (2000) *J. Biol. Chem.* **275,** 38659–38666
38. Bahouth, S. W., Sowinski, K. M., and Lima, J. J. (2001) *Biochem. Pharmacol.* **62,** 1211–1220
39. Carr, D. W., Stofko-Hahn, R. E., Fraser, I. D., Cone, R. D., and Scott, J. D. (1992) *J. Biol. Chem.* **267,** 16816–16823
40. Suvarma, N. U., and O'Donnell, J. M. (2002) *J. Pharmacol. Exp. Ther.* **302,** 249–256
41. Yuting, T., Hu, L. A., Miller, W. E., Ringstad, N., Hall, R. A., Pitcher, J. A., De Camilli, P., and Lefkowitz, R. J. (1999) *Proc. Natl. Acad. Sci. U. S. A.* **96,** 12559–12564
42. Coghlan, V. M., Perrino, B. A., Howard, M., Langeberg, L. K., Hicks, J. B., Gallatin, W. M., and Scott, J.D. (1995) *Science* **267,** 108–111
43. Wu, J., Ma, Q. N., and Lam, K. S. (1994) *Biochemistry* **33,** 14825–14833
44. Onorato, J. J., Palczewski, K., Regan, J. W., Caron, M. G., Lefkowitz, R. J., and Benovic, J. L. (1991) *Biochemistry* **30,** 5118–5125
45. Fredericks, Z. L., Pitcher, J. A., and Lefkowitz, R. J. (1996) *J. Biol. Chem.* **271,** 13796–13803
46. Freedman, N. J., Liggett, S. B., Drachman, D. E., Pei, G., Caron, M. G., and Lefkowitz, R. J. (1995) *J. Biol. Chem.* **270,** 17953–179561
47. Scott, J. D., Glauccum, M. B., Fischer, E. H., and Krebs, E. G. (1986) *Proc. Natl. Acad. Sci. U. S. A.* **83,** 1613–1616
48. Cao, T. T., Deacon, H. W., Reczek, D., Bretscher, A., and von Zastrow, M. (1999) *Nature* **410,** 286–290
49. Gage, R. M., Kim, K. A., Cao, T. T., and von Zastrow, M. (2001) *J. Biol. Chem.* **276,** 44712–44720
50. Gage, R. M., Matveeva, E. A., Whiteheart, S. W., and von Zastrow, M. (2005) *J. Biol. Chem.* **280,** 2205–3313
51. Hall, R. A., Premont, R. T., Chow, C. W., Blitzer, J. T., Pitcher, J. A., Claing, A., Stoffel, R. H., Barak, L. S., Shenolikar, S., Weinman, E. J., Grinstein, S., and Lefkowitz, R. J. (1998) *Nature* **392,** 626–630
52. Cong, M., Perry, S. J., Lin, F. T., Fraser, I. D., Hu, L. A., Chen, W., Pitcher, J. A., Scott, J. D., and Lefkowitz, R. J. (2001) *J. Biol. Chem.* **276,** 15192–15199
53. Fraser, I. D., Cong, M., Jim, J., Rollins, E. N., Daaka, Y., Lefkowitz, R. J., and Scott, J. D. (2000) *Curr. Biol.* **10,** 409–412
54. Fan, G.-F., Shumay, E., Wang, H.-Y., and Malbon, C. C. (2001) *J. Biol. Chem.* **276,** 24005–24014
55. Shih, M., Lin, F., Scott, J. D., Wang, H.-Y., and Malbon, C. C. (1999) *J. Biol. Chem.* **274,** 1588–1595
56. Malbon, C. C., Tao, J., Shumay, E., and Wang, H.-Y. (2004) *Biochem. Soc. Trans.* **32,** 861–864
57. Snyder, E. M., Colledge, M., Crozier, R. A., Chen, W. S., Scott, J. D., and Bear, M. F. (2005) *J. Biol. Chem.* **280,** 16962–16966
58. Vanhoose, A. M., and Winder, D. G. (2003) *J. Neurosci.* **23,** 5827–5834
59. Xu, J., Paquet, M., Lau, A. G., Wood, J. D., Ross, C. A., and Hall, R. A. (2001) *J. Biol. Chem.* **276,** 41310–41317
60. Hu, L. A., Chen, W., Martin, N. P., Whalen, E. J., Premont, R. T., and Lefkowitz, R. J. (2003) *J. Biol. Chem.* **278,** 26295–26301
61. He, J., Bellini, M., Inuzuka, H., Xu, J., Xiong, Y., Yang, X., Castleberry, A. M., and Hall, R. A. (2006) *J. Biol. Chem.* **281,** 2820–2827
62. Colledge, M., Dean, R. A., Scott, G. K., Langeberg, L. K., Huganir, R. L., and Scott, J. D. (2000) *Neuron* **27,** 107–119